The Pennsylvania State University

The Graduate School

Department of Meteorology

Case Studies Using GOES Infrared Data and a Planetary Boundary Layer Model to Infer Regional Scale Variations in Soil Moisture

A Thesis in

Meteorology

by

Fred G. Rose

Submitted in Partial Fulfillment

of the Requirements

for the Degree of

Master of Science

December 1983

We approve the thesis of Fred G. Rose.

Date of Signature:

_____	Toby N. Carlson, Professor of Meteorology, Thesis Advisor
_____	Alfred K. Blackadar, Professor of Meteorology, Graduate Faculty Reader
_____	John A. Dutton, Professor and Head of the Departmer Meteorology

ABSTRACT

Modeled temperature data from a one-dimensional, time-dependent, initial value, Planetary Boundary Layer (PBL) model for 16 separate model runs with varying initial values of moisture availability are applied, by the use of a regression equation, to longwave infrared GOES satellite data to infer moisture availability over a regional area in the central U.S.

This was done for several days during the summers of 1978 and 1980 where a large gradient in the Antecedent Precipitation Index (API) represented the boundary betweeen a drought area and a region of near normal precipitation.

Correlations between satellite derived moisture availability and API were found to exist. Errors from the presence of clouds, water vapor and other spatial inhomogeneities made the use of the measurement for anything except the relative degree of moisture availability dubious.

TABLE OF CONTENTS

TABLE OF CONTENTS (Continued)

LIST OF TABLES

LIST OF FIGURES

LIST OF FIGURES (Continued)

LIST OF FIGURES (Continued)

ACKNOWLEDGEMENTS

There are too many people who have contributed in one form or another to name them all, but I would like to give special thanks to:

Eileen Perry for doing the tedious and laborous work of locating and registering the nearly unrecognizable subgrids used in this thesis.

Toby Carlson, my thesis advisor, for his encouragement and motivation.

The McIdas facility at the University of Wisconsin, for supplying the GOES iamgery used in this thesis.

Walt Lottes and Fred Gadomski to whom I would run to on numerous occasions for help in computer-related problems.

This research was funded by a grant from the National Aeronautic and Space Administration (NASA) Grant #NAG-184.

1. INTRODUCTION

1.1 Purpose of this Thesis

Through history man has used his senses to make inferences about the processes about him. In the recent past these senses have been extended by the use of technology to include remote sensing of thermal radiation by orbital satellites. Just as an infant must learn to use his newly acquired senses, one must learn how to interpret this new wealth of thermal satellite data.

In this thesis case studies using Geostationary Operational Environmental Satellite (GOES) longwave infrared data will be used to determine the spatial and temporal evolution of soil moisture patterns. To accomplish these objectives an improved version of the Carlson-Boland, 1978; see also, Carlson et al., 1981 method for determining surface parameters will be used. Results in the form of surface moisture availability fields will be compared with analyses of antecedent precipitation (API) from rainfall data over the eastern Kansas regional area.

Soil moisture information is of use in a variety of ways. Crop yeild can be estimated by determination of drought severity. Moreover, in Numerical Weather Prediction (NWP) soil moisture information is necessary to improve the accuracy of a forecast, especially over meososcale regions, where an initialization of a moisture dependent surface heating parameter is crucial (Benjamin, 1983).

1.2 Soil Moisture Measuremement (An Overview)

The method used to generate imagery of soil moisture relies fundamentally on the observation that a wet surface will experience a lower maximum temperature and smaller morning temperature rise than a dry surface. This is the case for two reasons:

1) Evaporation

2) Specific Heat Capacity

When water evaporates it requires energy to accomplish the phase change. Radiant energy from the sun supplies this source. If there is a large availability of moisture at the surface this radiant energy will be used in evaporation, thereby allowing only a small rise in temperature.

The other physical factor is that water has a higher specific heat capacity than most soils. The presence of water in a soil gives that soil a larger thermal inertia (thermal property; Sellers, 1965) than one in a dry state. This causes the soil to give less of a temperature response to the solar forcing present. The result is that, once again, the rise in temperature for a moist surface is less than that for a dry surface.

In order to determine soil moisture, the ability to predict a surface temperature wave that corresponds to a specific soil moisture value is necessary. This task is undertaken by the use of a numerical model that will be discussed in a further chapter. Once information on temperature is predicted for values of moisture availability a quadratic regression equation is obtained from model output. By this means, moisture availability becomes a function of one or more of

several of the characteristics of the surface temperature wave predicted by the model. A more formal discussion on the correlation between these parameters and soil moisture will be presented later.

The surface temperatures corresponding to particular soil moisture values are taken from infrared radiometric measurements mode aboard one of several operational satellites, these satellites being:

a) Heat Capacity Mapping Mission (HCCM)

b) Geostationary Operational Environmental Satellite (GOES)

c) Tiros-N

d) NOAA-6,7

All of the satellites mentioned, except for GOES, are limited to making measurements near the times of maximum or minimum daily temperature. These satellites are in a low-level polar orbit and can record data with a high resolution. The HCMR (Heat Capacity Mapping Radiometer) aboard the HCCM satellite had the greatest resolution previously available (0.5 km). On the other hand, the GOES satellite with its VISSR (Visible Infrared Spin Scan Radiometer) has a poorer resolution (8 km) but can make frequent measurements from its 22,500 mile altitude over North America. This flexibility allows one to calculate a rate of temperature change which presumably contains information on soil moisture. Wetzel (1983) concluded that the use of GOES measurements to obtain a mid-morning temperature rise would be of value in determining a measure of soil moisture.

The radiometers aboard such satellites sense temperatures by the detection of electro-magnetic radiation near the wavelength of 10 microns, the atmospheric water vapor window. The energy in this

region corresponds to the peak in the frequency spectrum for bodies near a temperature of 288 degrees Kelvin. The determination of temperature in this way is by no means perfect. Emissivity of a surface varies with the material present. Moreover, the effect of atmospheric water vapor, with its own emission temperature, contaminates the measurement.

1.3 History of Previous Work

The measurement of soil moisture from satellites has been suggested by two basic means. Microwave sensing by both active and passive methods has shown some promise. Collection of soil moisture samples for test sites in Texas and Kansas were used in conjunction with Skylab microwave data by Eagleman (1975). Correlation coefficients were found to be between .40 and .75.

Much work using thermal infrared sensing to produce soil moisture information has been undertaken in the last five years. Rosema (1978) using the "Tell-US" algorithm applied aircraft IR data to determine surface relative humidity and thermal inertia. Price (1981) analyzed HCCM data to infer evaporative flux over Washington state using the "Tell-US" model to calibrate his own fourier component model. Recently, several authors including Wetzel-Atlas (1983) and Polansky (1982) made use of a boundary layer model in conjunction with the rate of morning temperature rise, measured from GOES data, to infer soil moisture over a regional-scale area. Both authors studied a similar area over the Great Plains, including eastern Kansas for July 1978. This area, which constitutes the focus of attention in this thesis, is

of interest because of drought situations which developed during the summers of 1978 and 1980. The drought was reflected by large gradients in API across Kansas present during most of the growing season.

This thesis is one of a series using the model originally developed by Carlson-Boland (1978) to aid in using satellite IR data to infer surface parameters, moisture availability, thermal inertia and the surface energy budget. Other additional research utilizing this model was done by Dodd (1979) who investigated Urban-Rural differences of surface parameters using HCCM data. Nocin (1979) studied small-scale surface moisture availability variability over a watershed using day-night HCCM pairs. Polansky (1982) investigated GOES data over two sites in Indiana and Kansas to determine the best times for use in morning temperature rise method.

2. THE MODEL

2.1 The Daytime Mode

The method used to generate moisture availability patterns requires the use of a one-dimensional, time dependent, initial value, boundary layer model. The model used was developed by Carlson and Boland (1978) and subsequently modified by Carlson et al. (1981). Further modifications since 1981 are described in the appendix. Surface temperatures as a function of time are simulated by the model for known values of moisture availability (M) and thermal inertia (P). Moisture availability can be defined as the ratio of actual evaporation to that of what could take place for a saturated surface. Since M controls the relative amount of evaporation taking place in the model, it also affects the partitioning of available radiant energy into latent heat. This results in different surface temperature wave simulations for the various M values. A numerical model must be used to produce surface temperatures that satisfy the solutions to the energy-balance equation

$$R_N = S(1 - A) + I_{dn} - I_{up} = H_o + LE_o + G_o \qquad (1)$$

2.2 Surface Layer Parameterization

The total incoming solar radiation (S) is calculated from a one-level radiative transfer model developed by Augustine (1977). I_{up} and I_{dn} are the upward and downward terrestrial radiation fluxes. These fluxes are functions of surface and atmospheric temperature as well as atmospheric water vapor content.

Sensible (H_o) and latent (LE_o) heat fluxes are parameterized by the use of eddy and molecular diffusivities as:

$$H_o = - (C_s + \rho C_s K_H) \frac{\partial \theta}{\partial z} \tag{2}$$

$$LE_o = - (\frac{L_E}{C_p} C_w + \rho L_E K_q) \frac{\partial q}{\partial z} \tag{3}$$

where K_h and K_a are the eddy diffusivities for heat and water vapor respectively. C_s and C_w are the molecular diffusivities for heat and water vapor.

In the model these diffusivities are described by resistance laws.

$$I_h = \int_0^{Z_A} \frac{dz}{(K_H + C_s/\rho\ C_p)} \tag{4}$$

$$I_w = \int_0^{Z_A} \frac{dz}{(K_w + C_w/\rho\ C_p)} \tag{5}$$

These equations describe integrals of the reciprocal of the combined eddy and molecular diffusivities which yield effective

resistances for the entire surface layer. K_h and K_w are parameterized by Monin-Obukhov scaling as:

$$K_H = \frac{ku_* z}{\phi_h} \tag{6}$$

$$K_w = \frac{ku_* z}{\phi_w} \tag{7}$$

$$u_* = \frac{u_A k}{\int_{z_0}^{z_A} \frac{\phi_m(z)}{z}\, dz} \tag{8}$$

where ϕ_h, ϕ_w, ϕ_m are the nondimensional stability parameters for heat, water vapor, and momentum. k is the Von-Karman constant, Z_o is the roughness length and U_A is the wind speed at the top of the surface layer (50 m). The functional forms for the stability parameters were given by Panofsky (1974). The integrals for the resistances I_h and I_w were solved by Benoit (1977).

These resistances are used to determine the fluxes of heat and moisture.

$$E_o = \frac{\rho L_E}{I_w} M(q_{os} - q_a) \tag{9}$$

$$H = \frac{\rho C_p}{I_L} (\theta_o - \theta_A) \tag{10}$$

where q_{os} is the surface saturation mixing ratio, q_a is the mixing ratio at 50 m, θ_o being the potential temperature at the surface, and θ_A being the potential temperature at 50 m. Here M is defined as the moisture availability which will be loosely associated wtih the true soil moisture.

The ground heat flux is given by the equation (Sellers, 1965):

$$G = \frac{\lambda(T_o - T_{-1})}{\Delta z} \tag{11}$$

T_o is the surface temperature,

T_{-1} is the temperature of the first substrate level below the surface, where λ is the thermal conductivity of the soil which is related to the thermal inertia (P) by

$$P = \frac{\lambda}{\kappa^{1/2}} \tag{12}$$

with κ being the thermal diffusivity of the soil. A regression equation was derived between P and λ by Dodd (1979) in order to specify

unique values of lambda (λ) and kappa (κ) for a given P. It was determined by regression for a wide range of soils and materials that:

$$\lambda = -0.00013 + 0.050502P + 1.21P^2 \tag{13}$$

this equation was found to explain 91% of the variance of λ about P. The flow of heat through the soil is taken into account in the diffusion equation (Sellers, 1965)

$$\frac{\partial T}{\partial t} = \kappa \frac{\partial^2 T}{\partial z^2} \tag{14}$$

Finally, equations (1), (9), (10), (11) are combined to produce an expression for sensible heat flux and surface temperature.

$$H_o = \frac{R_N - \frac{\rho L_E}{I_w} M (q_{os} - q_A) - \frac{\lambda}{\Delta z} (\Gamma z_A + T_o - T_{-1})}{1 + \frac{\lambda I_h}{\Delta z \rho C_p}} \tag{15}$$

$$T_o = \theta_o = \Theta_A + \frac{HI}{\rho C_p} \tag{16}$$

These expressions are solved in the model, for a time step of 240 seconds, to determine a new surface temperature.

2.3 The Mixed Layer

The surface heat flux also governs the growth of the mixed layer according to the method described by Tennekes (1973). The growth of the mixed layer is partially dependent upon the entrainment of air with the larger potential temperature from above the mixed layer.

Until recently the model held the wind speed at the top of the surface layer constant. Improvements to the model now allow wind speed to be predicted at several levels within the mixed layer. These modifications are documented in the appendix.

2.4 The Nighttime Mode

In the nighttime mode of the model ($H_o < 0$) the physics used in the daytime mode ($H_o > 0$) is inappropriate because of the insignificance of turbulent mixing. The integrals for the resistances would diverge to infinity as radiational cooling processes predominated producing a stable, quiescent atmosphere. Therefore, in the nighttime mode we choose our computational scheme as a function the bulk Richardson number (B), which is a measure of stability in the surface layer. The bulk Richardson number is defined as:

$$B = \frac{gZ_A}{\overline{\theta} w_A} \left[(\theta_A - \theta_1) + T_* \ln \frac{z_A}{z_o}\right] \qquad (17)$$

where g is gravity, $\overline{\theta}$ is the average potential temperature of the surface layer, w_a is the wind speed at height z_a, (50 m), θ_a is the potential temperature at Z_a, θ is the potential temperature at a height 1.3 meters above the surface.

In order to compute heat flux (H_o) we once again utilize Monin-Obukhov scaling to define H_o in terms of U_* and T_*.

$$T_* = \frac{(\theta_A - \theta_1)}{(\ln(\frac{z_1}{z_o}) - \psi_h)} \tag{18}$$

$$u_* = \frac{k\ W_A}{(\ln(\frac{z_1}{z_o}) - \psi_m)} \tag{19}$$

$$H_o = -k\ \rho\ c_p\ u_*\ T_* \tag{20}$$

where ψ_h and ψ_m are nondimensional corrections dependent on stability.

From the bulk Richardson number we define three stability classes and associated modes of computation.

$B < 0$	unstable
$0 < B < 0.2$	stable
$B > 0.2$	nonturbulent

The entire nighttime mode of the model is a close adaptation of the model developed by Blackadar (1979). A more detailed description of the nighttime model physics may be found in a thesis by Dodd (1979). The following is a physical description of how the model proceeds through the three stability classes as the evening progresses.

In its present form, when the model leaves the daytime mode (i.e., $H_o < 0$), it never returns to it. To account for fluctuations near this time of "radiation sunset" the unstable computational mode allows for transient periods of positive heat flux. As the evening progresses the stable mode is entered, the surface temperature drops and the wind speed at the top of the surface layer decreases due to the lack of momentum transfer from the increasingly stable levels above the surface layer. Heat flux in the stable mode is negative driven through the mechanical turbulence present. Since the stable temperature profile allows only a minimal amount of momentum transfer from upper layer winds, surface friction predominatres causing the lowest level winds to decrease to a point where $B > 0.2$.

Once in the non-turbulent mode u_* and H_o are set to zero. In this mode surface temperature is computed to set the balance between outgoing longwave radiation and heat flux leaving the soil. Thus:

$$R_N = G$$

$$\varepsilon_g T_g^4 - \varepsilon_a \sigma T_a^4 = \lambda \frac{\partial T}{\partial z} \qquad (21)$$

During the night, the winds above the surface layer experience an inertial oscillation due to the coriolis effect. Shear between the upper models levels may increase to cause a destabilization ($R_i < 0.2$) and mix momentum to the surface layer. The increase of wind speed at the lowest level could bring the bulk Richardson number below 0.2

causing the model to enter the stable mode. Once in the stable mode, negative heat flux will result in an increase in surface temperature. The increase of turbulence and surface friction decreases wind speeds to bring the model, once again, into the nonturbulent mode. Under appropriate conditions several of these "turbulent interludes" may occur during the night.

3. APPLICATION OF MODELED TEMPERATURE DATA TO SATELLITE IMAGERY

3.1 Correlation Techniques

At present there are four similar techniques by which soil moisture information can be extracted from the model output. All of these techniques use the assumption that the diurnal temperature wave at the surface is noticeably affected by moisture availability. Most notably, moisture availability has been found to affect the maximum afternoon temperature and morning temperature rise (Wetzel and Atlas, 1981).

The first correlation technique used in conjunction with modeled surface temperatures was first applied to HCCM IR imagery. This technique was the so-called DAY-NIGHT method, since times of satellite overpass were at 2 AM and 2 PM (Carlson and Boland, 1978; Rosema, 1978; see Dejace et al., 1979). These times corresponded roughly to those of maximum and minimum diurnal temperature. Several separate runs of the model using differing initialization values were made. In regressing M upon the two predictors, it was found that the daytime coefficients in the regression equation were the most significant in the determination of a moisture availability. The analysis of T-ratios* were used to interpret significance. For all of the regressions using the "Day-Night" technique the T-ratios for the nighttime coefficients were

*The term "T-ratio" describes the confidence limit for a given coefficient in the regression equation. For a quadratic regression equation in two variables (11 deg. freedom), as in the "Day-Night" technique, the T-Ratio corresponding to a 95% confidence interval is 2.20.

well below 2.2 indicating that little "information" on moisture availability was obtained from the use of the nighttime (2 AM) temperature image. However, the T-Ratios for the 2 PM (Day) temperatures were significantly above 2.0 indicating that most of the "information" in the DAY-NIGHT method came from the daytime temperature image. Conversely, fields of derived thermal inertia extracted most of their "information" (large T-Ratio) from the 2 AM (Night) temperature image.

The second technique involved using three temperature images so that two temperature difference fields could be found. This technique, invented by Polansky (1982), can, at present, only be applied to GOES data because of the satellite's ability to take measurements at half-hour intervals. The two temperature difference fields used in this technique are found between a mid-morning time (0800 local) and an early afternoon time (1300 local), the second difference is taken between a nighttime image (0200 local) and the same afternoon image. Polansky (1982) ran extensive sensitivity tests to determine that these times corresponded to those with the best correlation for moisture availability and thermal inertia. One of the problems with the three image method is the contamination of the imagery by clouds. If the area of interest is obscured by clouds for any of the three times a measure of soil moisture will be undeterminable. The appearance of clouds makes the use of this technique difficult for all but a few clear weather situations experienced at a particular location. In order to allow soil moisture to be measurable on a more frequent basis and since information is obtainable without the use of a nighttime

image, a technique was developed using only the mid-morning and the afternoon temperature images.

This third technique makes use of a correlation on the morning temperature rise which is obtained from differencing of the mid-morning and afternoon images (Wetzel and Atlas; 1981, 1983). The morning temperature rise technique also regresses upon the modeled afternoon temperature to produce a quadratic equation expressing moisture availability in terms of two variables, temperature rise and afternoon temperature. This techique was used to produce moisture availability fields for five cases in this thesis.

On a few occasions the mid-morning image was obscured by cloud to a sufficient extent to force it to be discarded. Considering that most of the spatial variation in temperature occurred in the afternoon (i.e., most of the signal) and that spatial variations in the morning temperature image were in many cases comparable to the "noise" (see chapter on errors) found in the afternoon image, a fourth technique is used in which correlates soil moisture is correlated with the afternoon temperture alone. In this rather simple technique, afternoon temperatures from the GOES satellite were one on one mapped into moisture availability values. This was done with a regression equation obtained by regressing only the afternoon modeled temperature on moisture availability.

3.2 Conversion of Model Output

All of the previously mentioned techniques rely on model output from 16 separate runs where initialization of the model is the same except that values of M and P are varied. In previous studies by Dodd

(1979), Kocin (1979) and Polansky (1982) model runs were made using all combinations of the four values of each variable M and P (see Figure 1).

In order to describe the temperature response characteristics to soil moisture more accurately, the exclusion of some of the unrealistic combinations of M and P (i.e., "low P, high M"; and to a lesser extent "high P, low M") were made in favor of using more values of M. This was done by using seven values of M and four values of P in a staggered arrangement so that the unrealistic pairs are omitted (see Figure 2).

The use of seven values allows variations in the temperature response due to M to be explained by the regression equations to a a greater degree of accuracy, especially at low values of M where modeled temperature response is highly sensitive to variations in M.

3.3 Sensitivity of Temperature Response

The sensitivity of modeled temperature response to M is variable from case to case. One of the most important influences on sensitivity is atmospheric humidity. If a humid atmosphere is present over the area of study the modeled temperatures will be similar over all but the driest values of M. This will be the case because temperature variations due to M are brought about through differences in the partitioning of radiant energy into latent heat. In a humid atmosphere surface evaporation will be small regardless of the moisture availability.

Another influence on sensitivity is wind speed (Wetzel and Atlas; 1981, 1983). Under windy conditions the increased turbulence allows greater fluxes of both sensible and latent heat into the atmosphere.

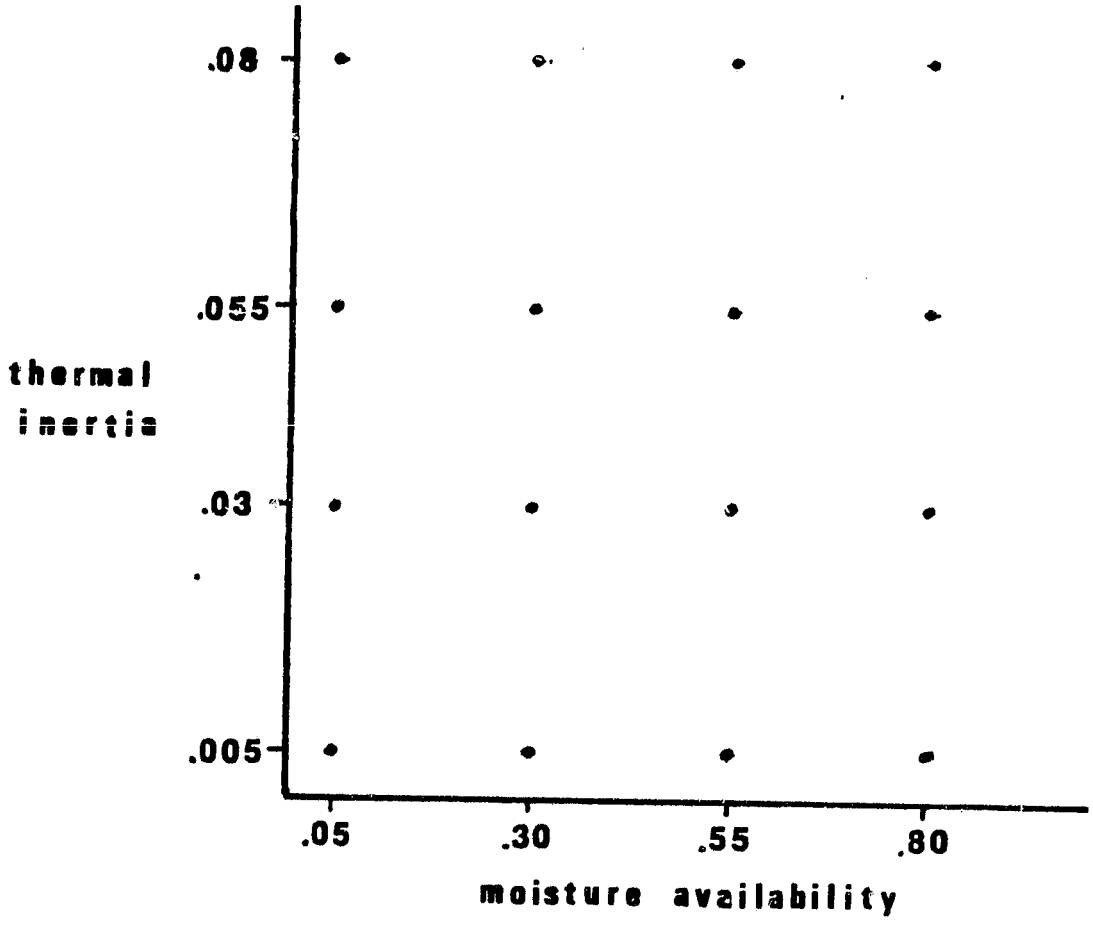

Figure 1. Points indicate the M and P pairs used by Dodd, Kocin, Polansky for the 16 model runs from which regression equations for M and P were obtained.

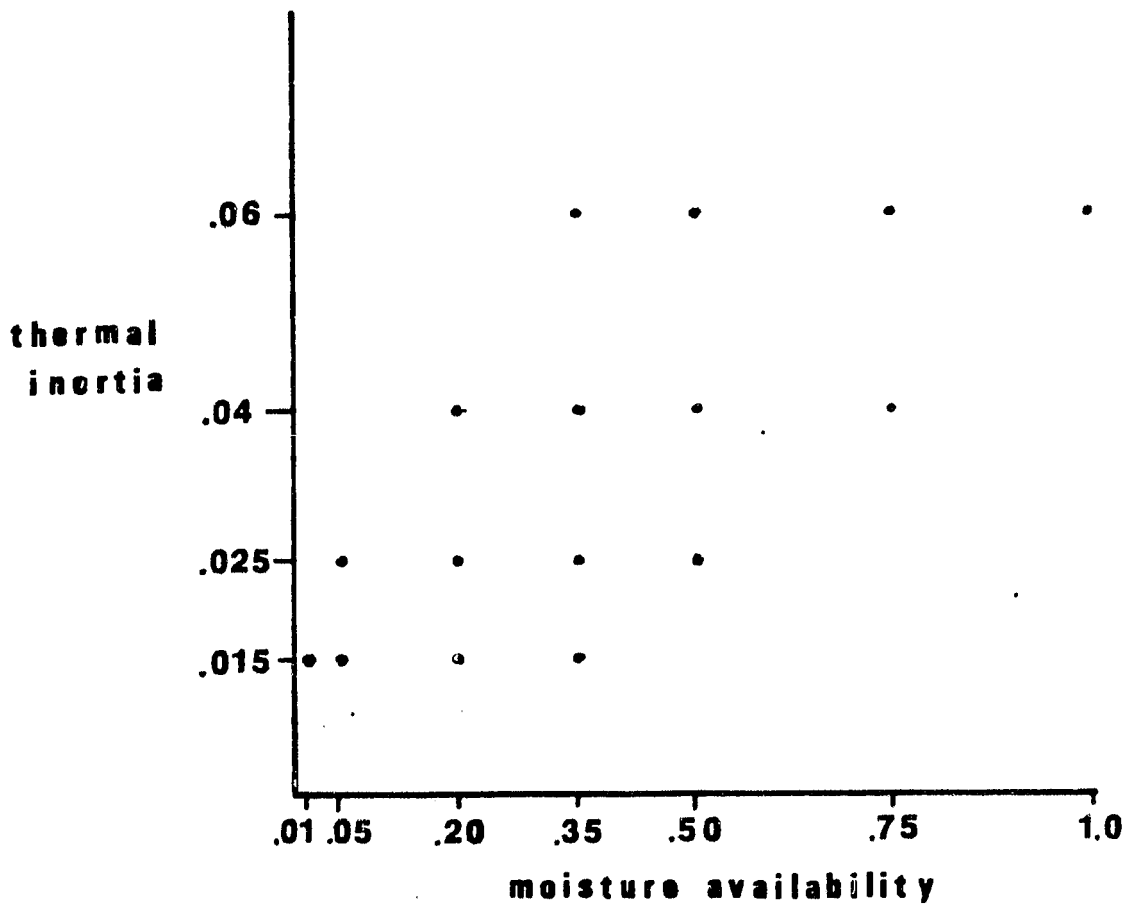

Figure 2. Initialization of 16 M and P pairs used in this thesis Physically unrealistic pairs of low thermal inertial and high moisture availability are omitted.

The large fluxes reduce the amplitude of the surface temperature response making the correlation with soil moisture more susceptible to errors from temperature variations from other sources. These sources of error will be discussed in a later chapter. Windy conditions switch the main controlling parameter of temperature response from moisture availability toward that of roughness. Here a rough surface will produce more mechanical turbulence than a smooth surface allowing a lower surface temperature to be maintained as a result of greater heat fluxes.

The application of a regression equation from modeled temperatures allows the satellite-derived IR temperatures to be converted to a measure of soil moisture, the parameter M. Clearly, the simplest relationship between afternoon temperature and soil moisture would be a linear one. In this case the lowest afternoon temperature within the image might correspond to a moisture availability of 1.0. At the other end of the temperature range a large temperature, corresponding to no latent heat flux, gives a moisture availability value of 0.0. Under most conditions there is sufficient amtospheric humidity and surface wind speed to make the relationship between temperature and moisture availability depart from linear.

The results of several model runs show that a derived soil moisture value is very sensitive to the measured temperature where low surface temperatures are present. This makes the assessment of soil moisture over wet (low temperature) regions more subject to errors in surface temperature. These model runs suggest that a greater accuracy

in the resolution of soil moisture is possible over drier, desert-like, regions. However, this conclusion may be tempered by observations showing that a rapid and large temperature response may occur over the low thermal inertial soils of desert-like regions. Fast response may subject the results to error from forcing by small-scale variations.

4. RESULTS

4.1 Location of Study

The area used for this case study (see Figure 3) consists of approximately 130,000 km^2 including most of eastern Kansas and a portion of southern Nebrasks. Most of the land in this region consists of cropland or grazing land. A map of land use is shown in Figure 4. The map background used in Figures 5-52 shows cities (represented by capital letters), rivers, lakes, and state boundaries. The Kansas area was chosen for several reasons. Elevations throughout the area are rather uniform varying from 500 ft in the broad river valleys in the east to near 1000 ft in the western portion of the study area. Large water bodies are absent in this area making the assumption of a homogeneous air mass more likely. However, the most prominent reason for choosing this area was that a large gradient in soil moisture, due to rainfall variations, was present through the area during the summers of 1978 and 1980. It is expected that a correlation between the results obtained by the GOES satellite and the analysis of API will be found.

4.2 API Analysis

In order to obtain an objective measure of soil moisture that can be compared to satellite-derived results, rainfall data were used to produce an Antecedent Precipitation Index (API) field for each of the days in the study. API is a measure of rainfall that puts a temporal

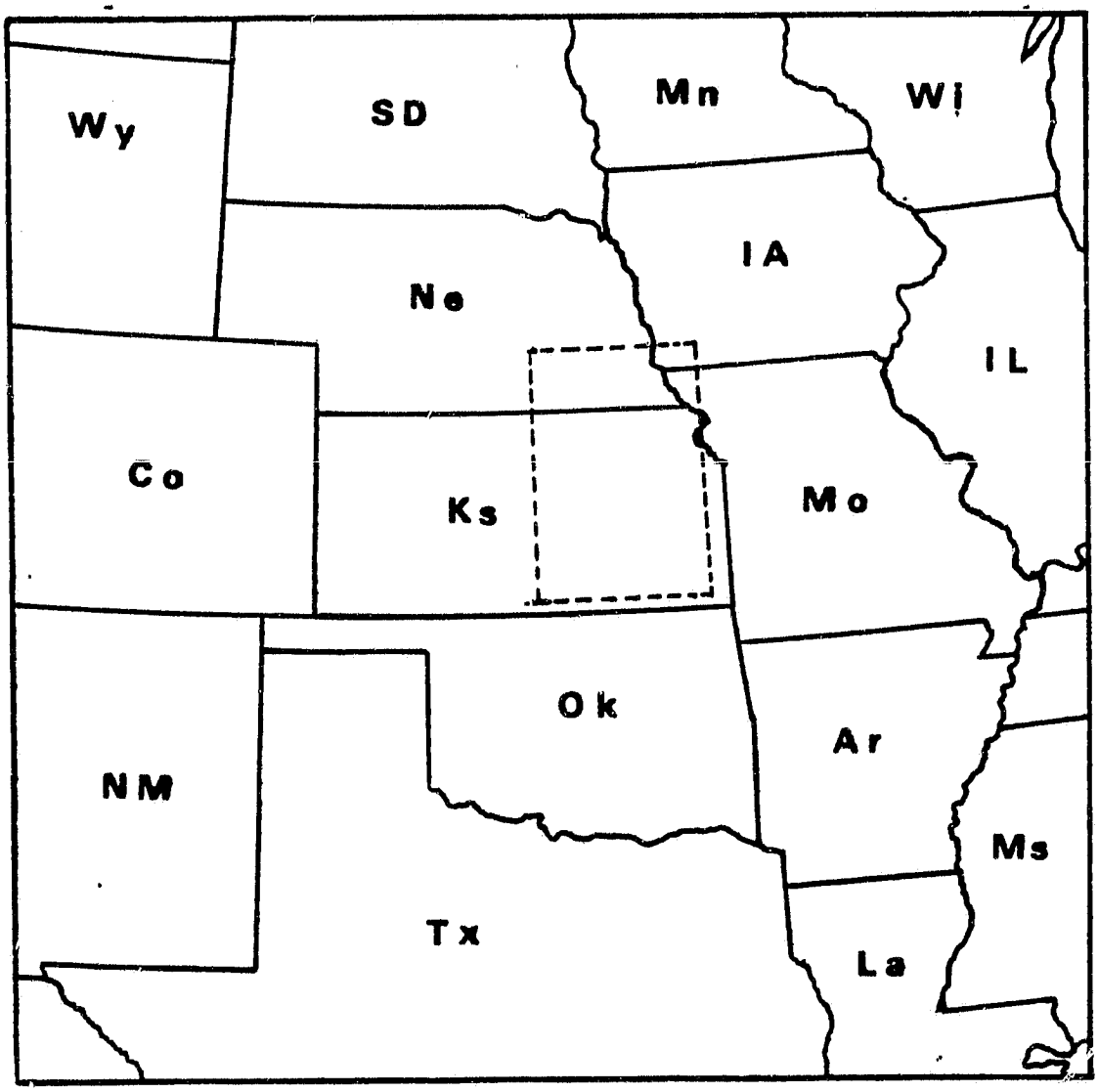

Figure 3. Location of case study area.

Land use/land cover for study area

1) Mostly cropland
2) Cropland with grazing land
3) Cropland with pasture, woodland and forest
4) Irregated land
5) Woodland, forest with some cropland and pasture
6) Urban
7) Lakes and rivers
8) Subhumid grassland and semi-humid grazing land

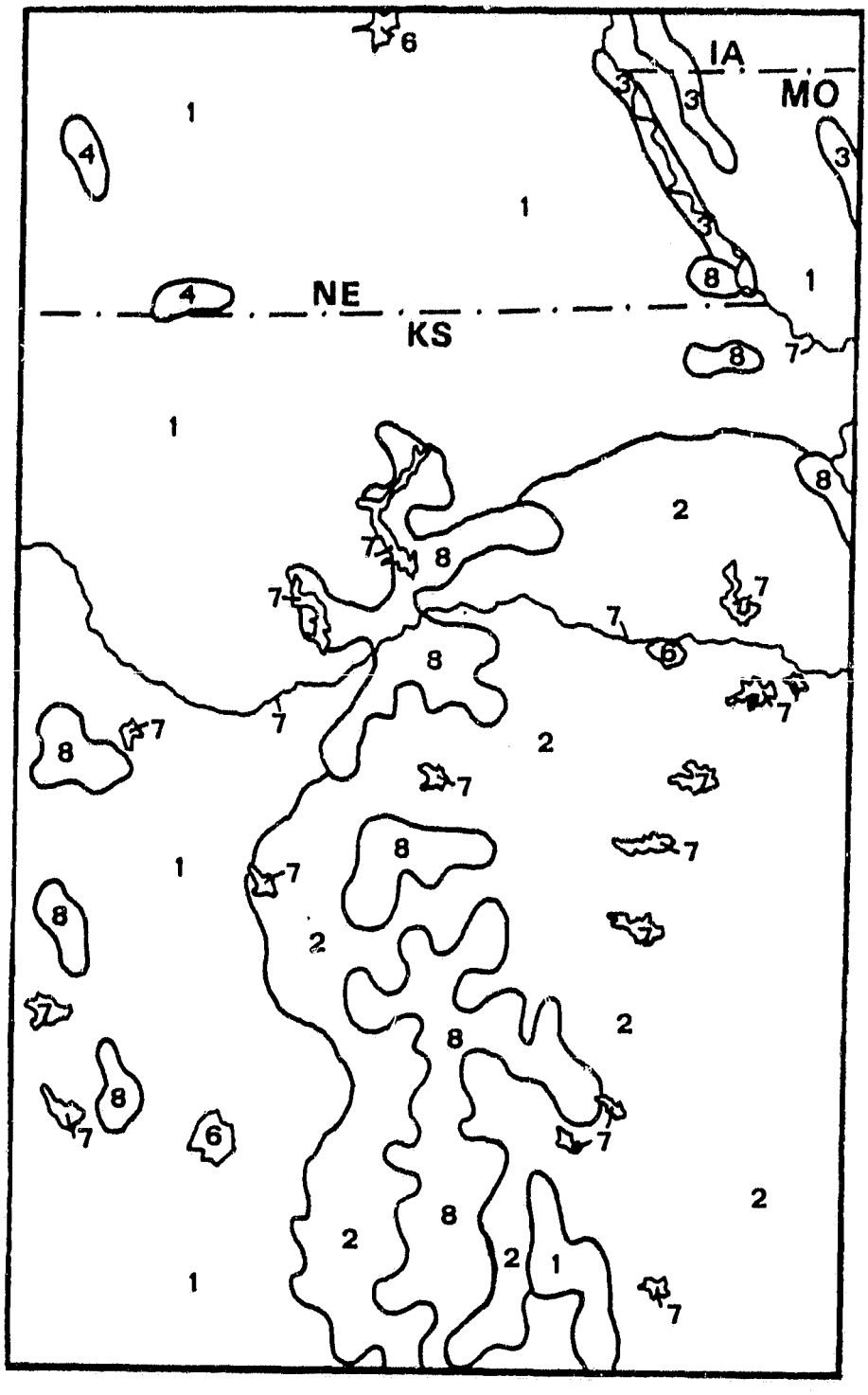

Figure 4. Land use/land cover for study area.

weighting on the precipitation events occurring within the time scale of a few weeks. In this way, the process of "drying out" after a large rainfall event can be represented. The API computation is expressed by:

$$API_i = k \times API_{i-1} + Rainfall_i \qquad (22)$$

where API_i is the index value for the present day, API_{i-1} is the value for the previous day, k is the weighting coefficient that determines the rate of "drying out." A k coefficient of 1.0 would imply that no drying should occur while a value of zero for k would negate the influence of any past rainfall on that day's API value. The k value chosen in this study is 0.92. This value was chosen on the basis of a study by Saxton (1967). The k coefficient is a factor of some concern since it is an empirically determined coefficient that is a function of several spatial and temporal variables. Soil type, vegetation, insolation, rooting depth of the vegetation, and rainfall runoff are some of factors that control the API weighting value.

Another factor that influences the analysis of API made in this thesis is the sparse network of stations reporting rainfall. The average spacing between the 44 locations used was approximately 100 km. The source of the daily rainfall data is from NOAA Environmental Data and Information Service at the National Climatic Center in Asheville, NC. This mismatch in scale (8 km -satellite, 100 km -API) along with the stochastic nature of rainfall makes errors due to the resolution of a rainfall event likely. So in practice API cannot be thought of as a

direct measure of soil moisture; instead it is a course indicator of degree of aridity that does not consider sources of water other than rainfall such as irrigation, ground water, rivers.

A log scale was used for the API values in the correlation with moisture availability. In this way extremely large values, where the soil has reached saturation, are compressed while the dryer smaller values of the API index are relatively expanded to show more effectively the variations in soil moisture below field capacity. This log scale has been divided into arbitrary categories for easier recognition. The driest (n = 0) category is based on a very dry API value of 0.12 inches. Each doubling of the API base value of 0.12 represents one category in the LOG API index.

To convert API values into the LOG API values used for this thesis the following relationships are valid:

$$API = 0.125\ (2^n)$$

$$n = [\ln(API) - \ln(0.125)]/\ln(2.0)$$

In subsequent figures, log API refers only to the exponent number (n).

The method used to extract data points from the subjective API analysis and the satellite derived moisture availability fields consisted of subjective determination of values at 104 grid points in an 8 x 13 configuration over the study area. Some of the values were rejected if they were thought to be influenced by a region of cloud cover. The remaining data pairs were regressed upon to obtain an equation expressing the LOG API value in terms of a moisture availability value.

4.3 Cases Using the Morning Temperature Rise Technique

4.3.1 July 15, 1978

The day of July 15, 1978 was relatively cloud-free except for an area near Wichita in the afternoon (19 Z) and a band of clouds along the southern boundary in the morning (14 Z). The afternoon (00 Z) soundings from the Topeka station, which is the site for all of the soundings used in this study, revealed humidities in the 50-60% range, near the surface, with a light 4 kt northerly wind. The analysis of morning (14 Z) and afternoon (19 Z) temperature images, as well as the analyses of derived moisture availability (M) and API, are shown in the following figures. As discussed in Section 3.3, the low wind speeds and humidities present in this case help to give the best correlation between M and API for this technique, an R^2 value of 0.73.

4.3.2 July 27, 1978

The sounding for the July 27, 1978 case reveals more low level mositure than for the July 15 case. Wind speeds during the day were 4-6 kts from the north. However, observation of visible satellite photos and synoptic data reveal the presence of a thin layer of cirrus clouds over the northeast portion of the area for both the 1430 Z and 2000 Z images. There is no sharp gradient in temperature to reveal these areas of cirrus clouds. This makes the separation between contaminated data and acceptable data difficult. The effect of these cirrus clouds along with the higher amounts of low-level moisture reduce the accuracy of the soil moisture estimate. The correlation between API and M in this case gives an R^2 value of 0.39.

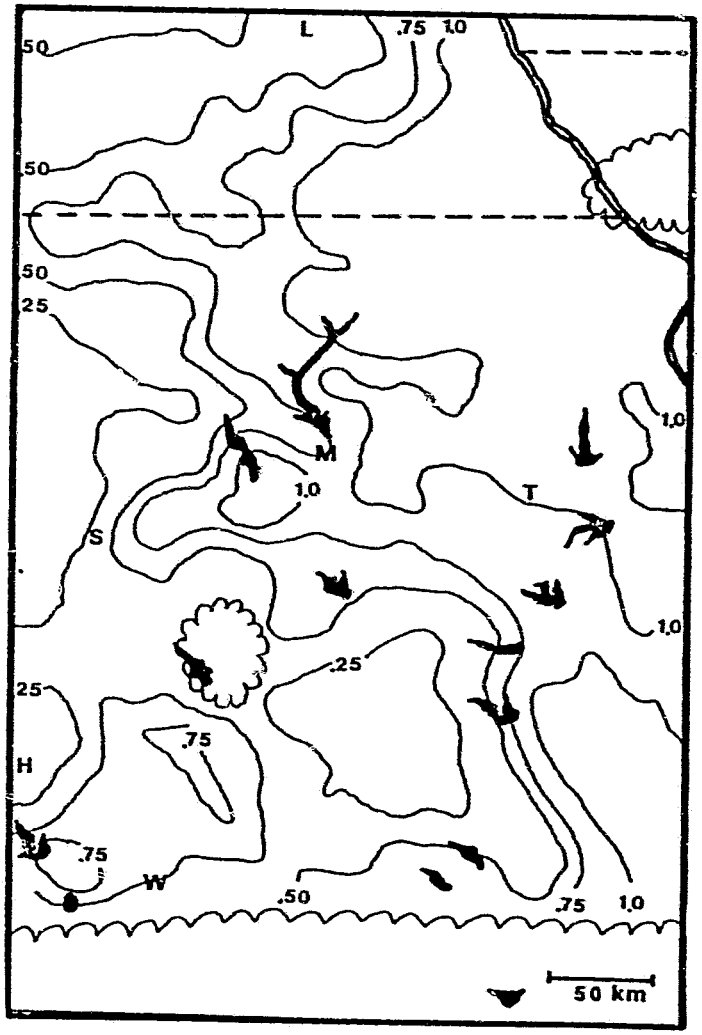

Figure 5. July 15, 1978 moisture availability.

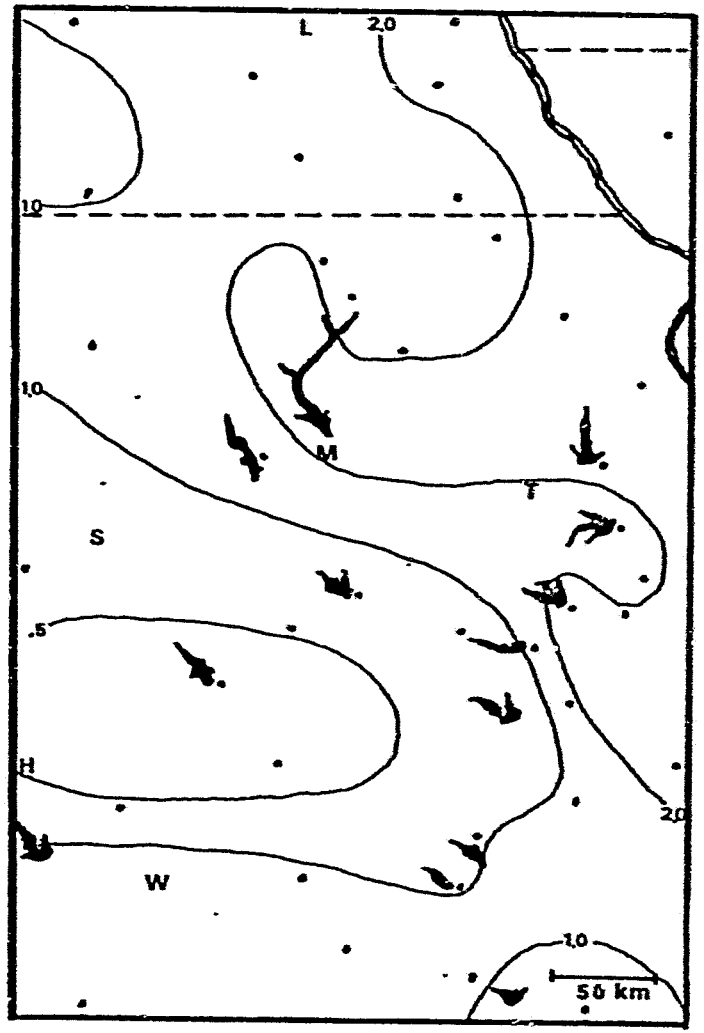

Figure 6. July 15, 1978 API analysis.

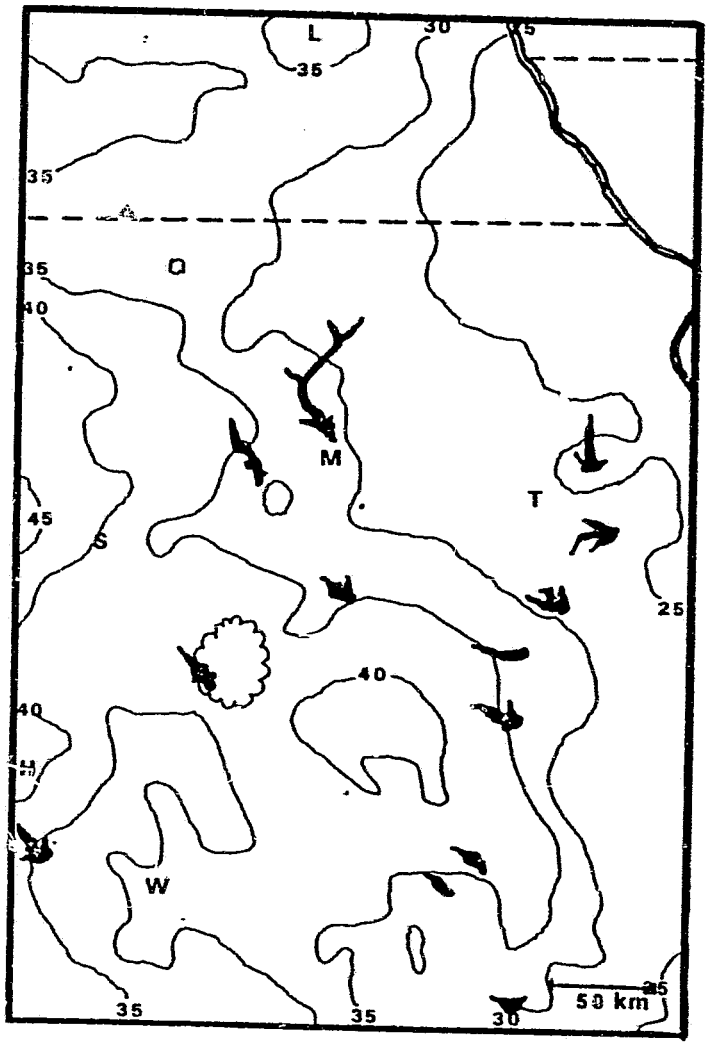

Figure 7. July 15, 1978 afternoon temperature (1900 z).

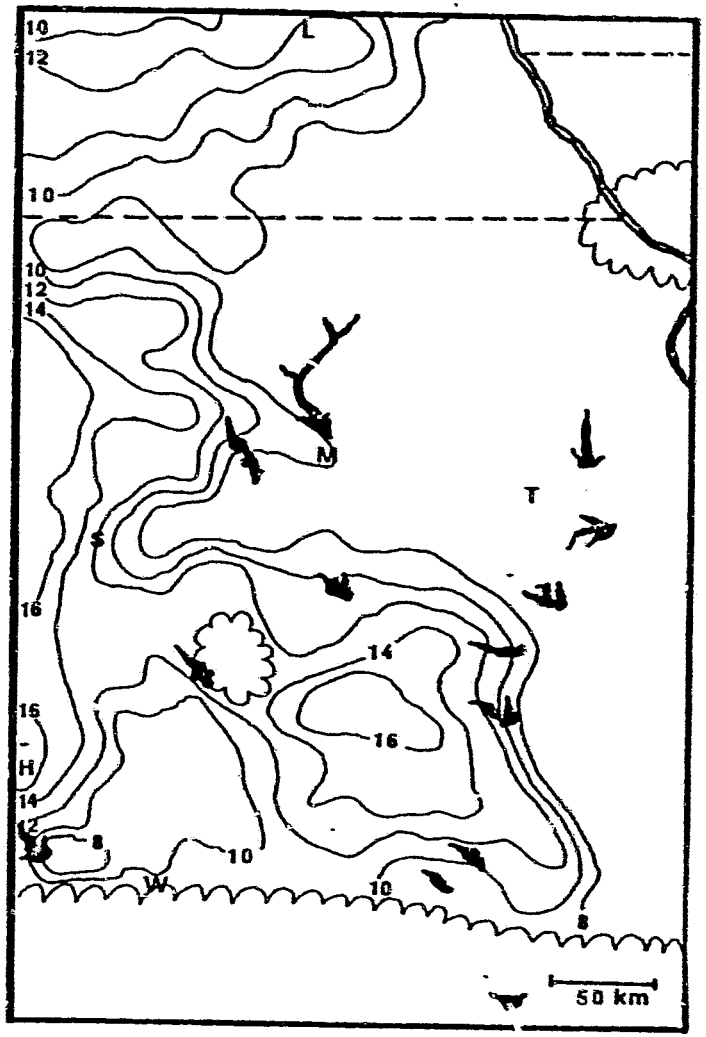

Figure 8. July 15, 1978 morning temperature rise (1900 - 1400 z).

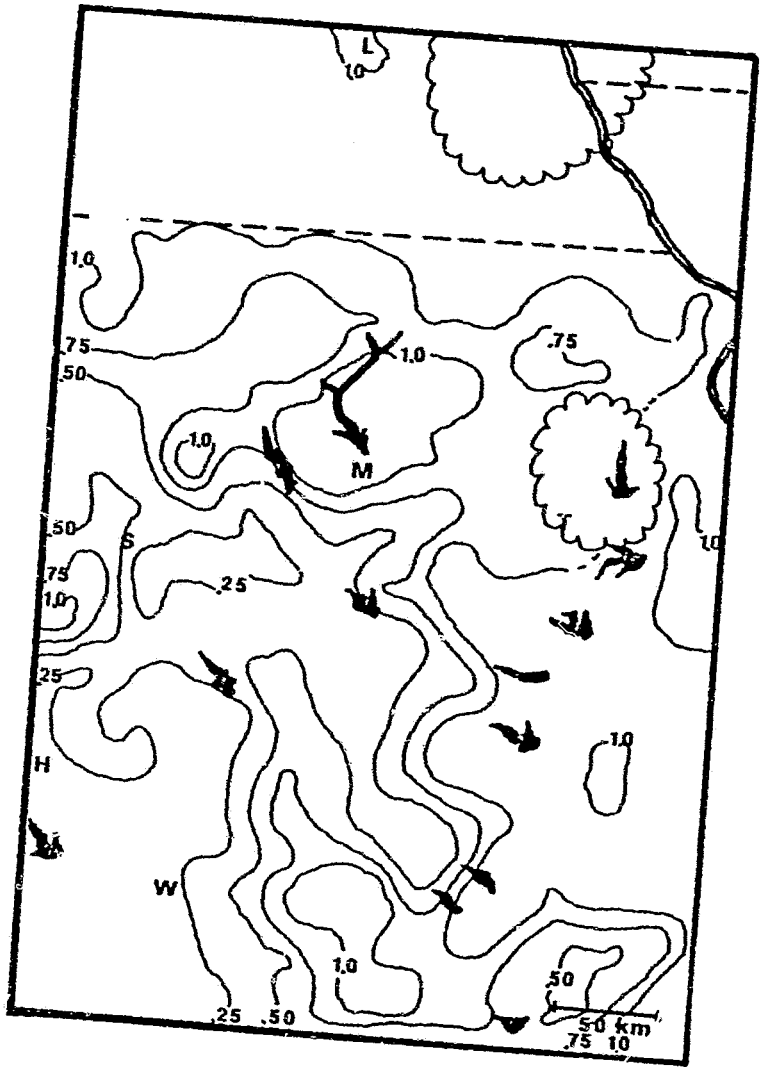

Figure 9. July 27, 1978 moisture availability.

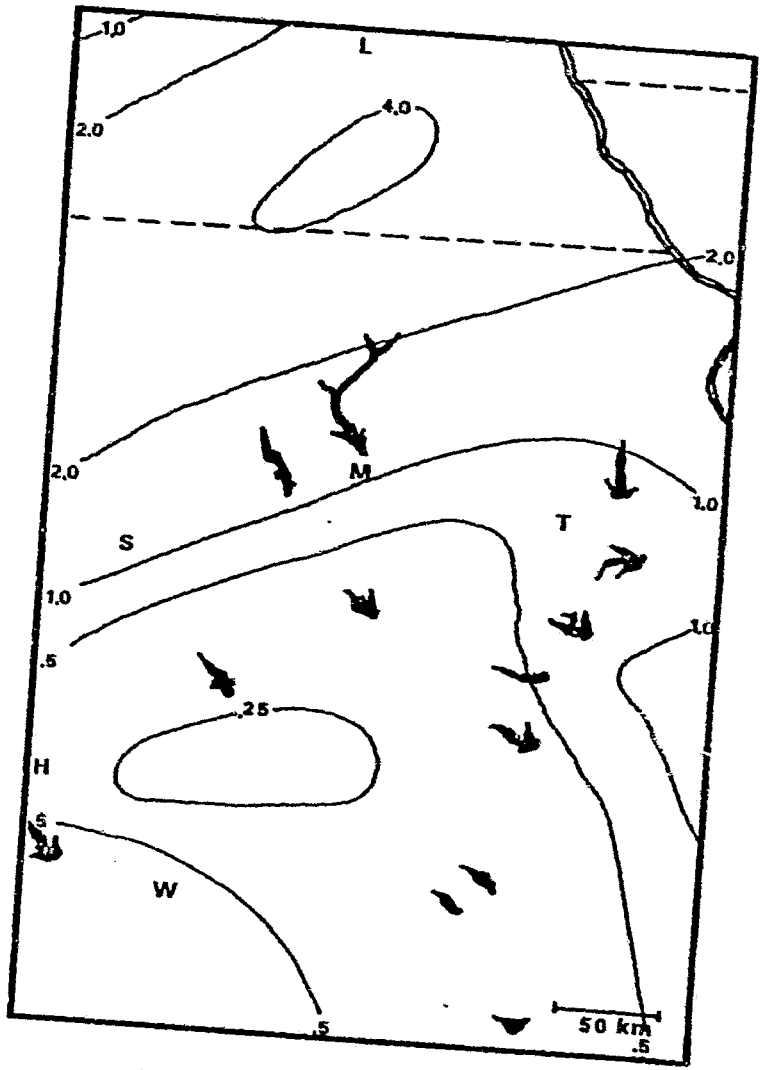

Figure 10. July 27, 1978 API analysis.

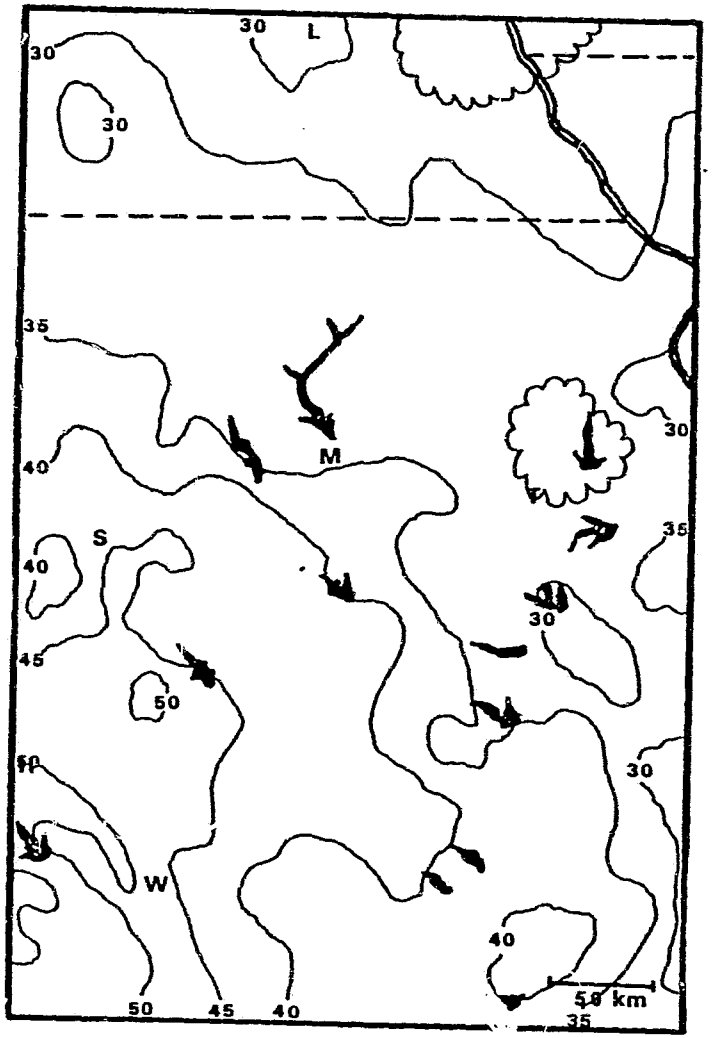

Figure 11. July 27, 1978 afternoon temperature (2000 z).

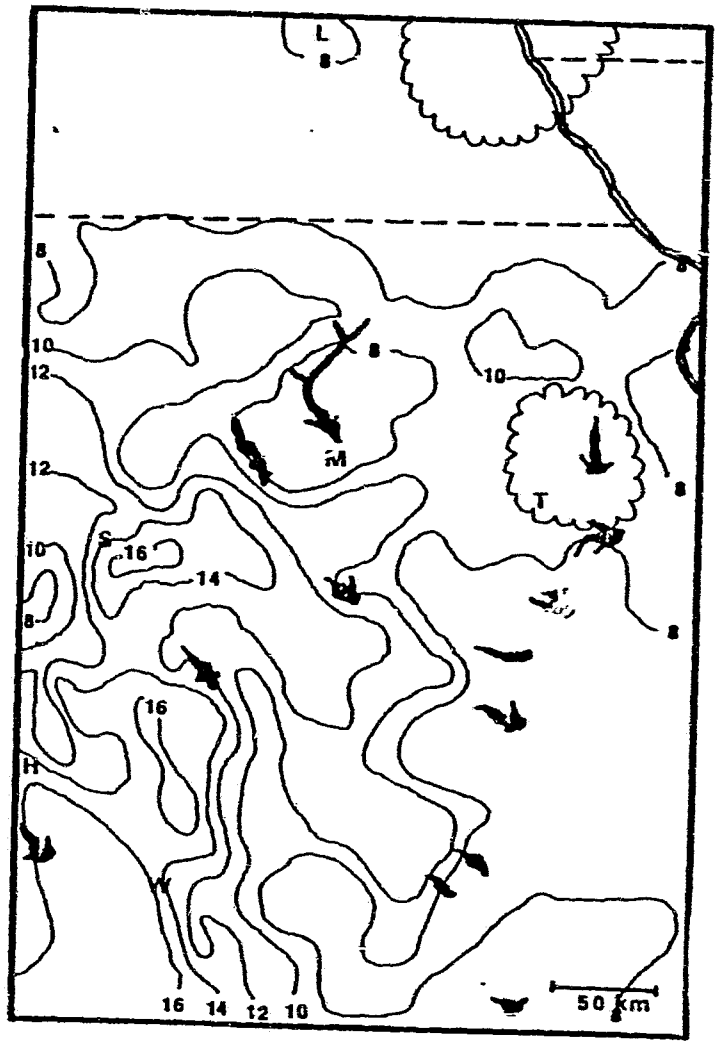

Figure 12. July 27, 1978 morning temperature rise (2000 - 1430 z).

4.3.3 July 1, 1980

A cold front was present on this day across the northern portion of Kansas making the requirement of homogeneity of air masses invalid. Winds in southern Kansas were light from the southwest, while strong northeast winds were present over northern Kansas and Nebraska. Also, a temperature gradient existed which could be seen in an analysis of synoptic data.

The presence of this cold front makes analysis of moisture availability invalid. This is clearly represented by the very low R^2 value of 0.04 between M and API.

4.3.4 July 14, 1980

Humidities encountered on this day were in the 20-30% range over the study area. These dry conditions make the detection of soil moisture more reliable because a greater variation of evaporation and surface temperature are allowed in a dry atmosphere. However, a rather strong southewesterly wind at 10-15 kts reduced the overall amplitude of temperature variation, as compared to a weak wind case, a situation which increased the susceptibility of soil moisture measurement to error. Clouds obscured measurement over small areas in Nebraska for the morning (14 Z) image. Overall the R^2 of the July 14 case was 0.63.

4.3.5 August 23, 1980

The sounding for August 23, 1980 revealed rather high humidities (50-70%) within the lower 50 mb of the atmosphere. Winds were

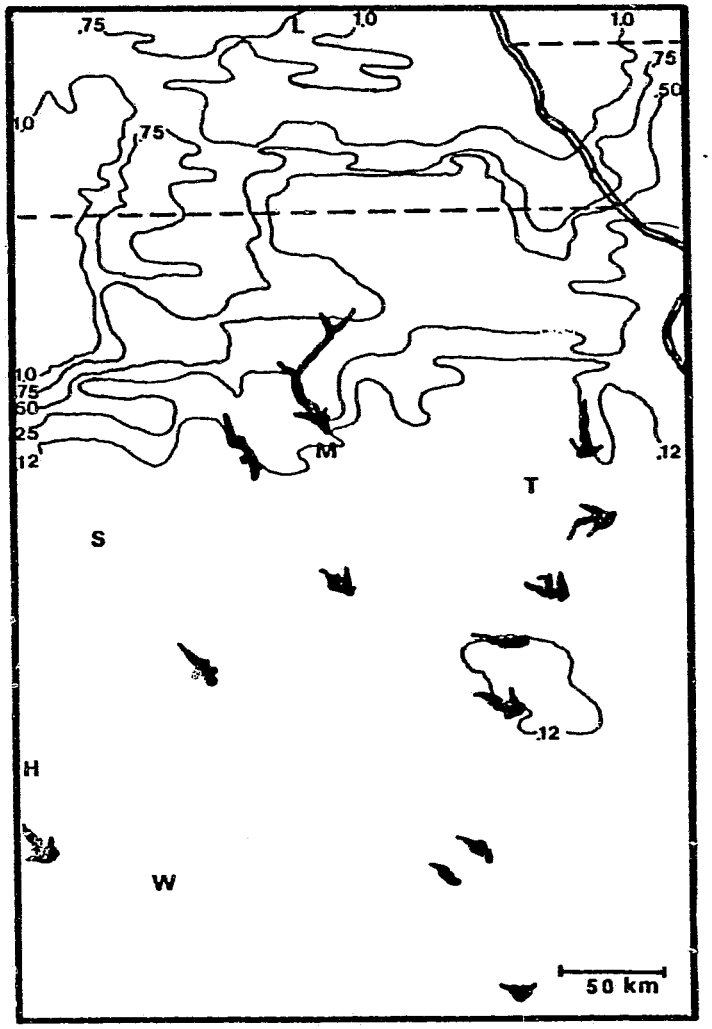

Figure 13. July 1, 1980 moisture availability.

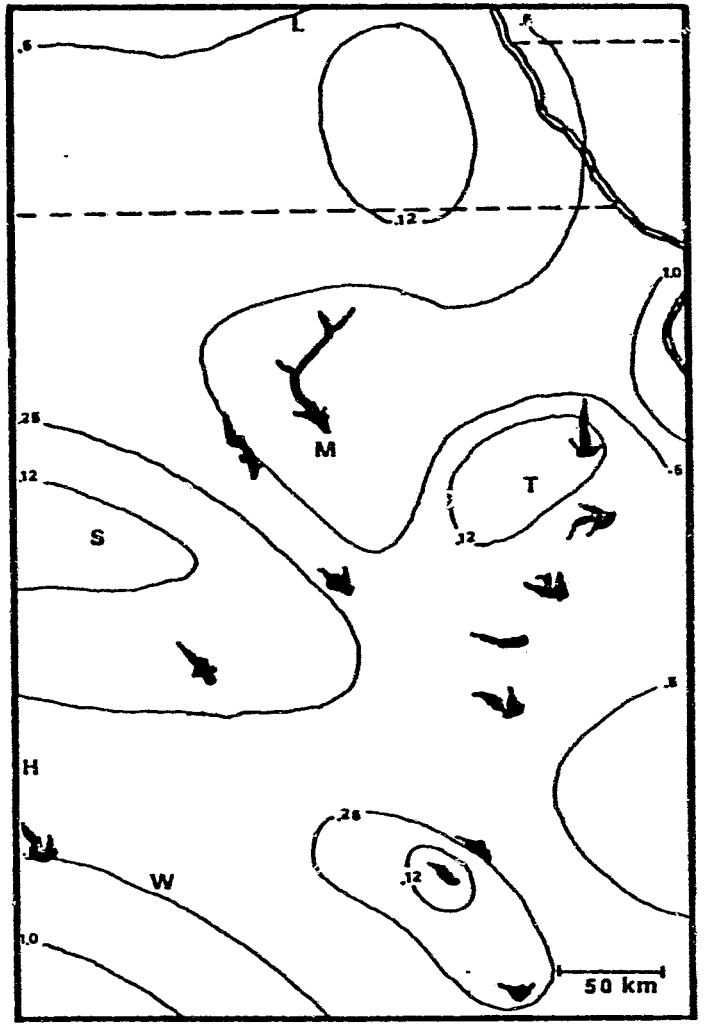

Figure 14. July 1, 1980 API analysis.

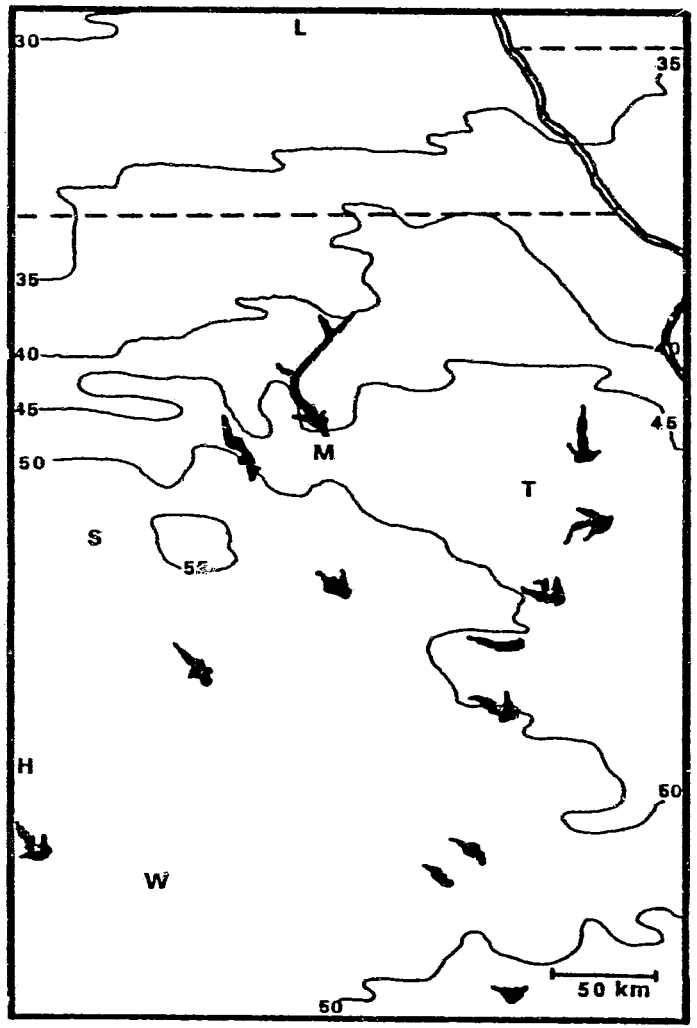

Figure 15. July 1, 1980 afternoon temperature (2000 z).

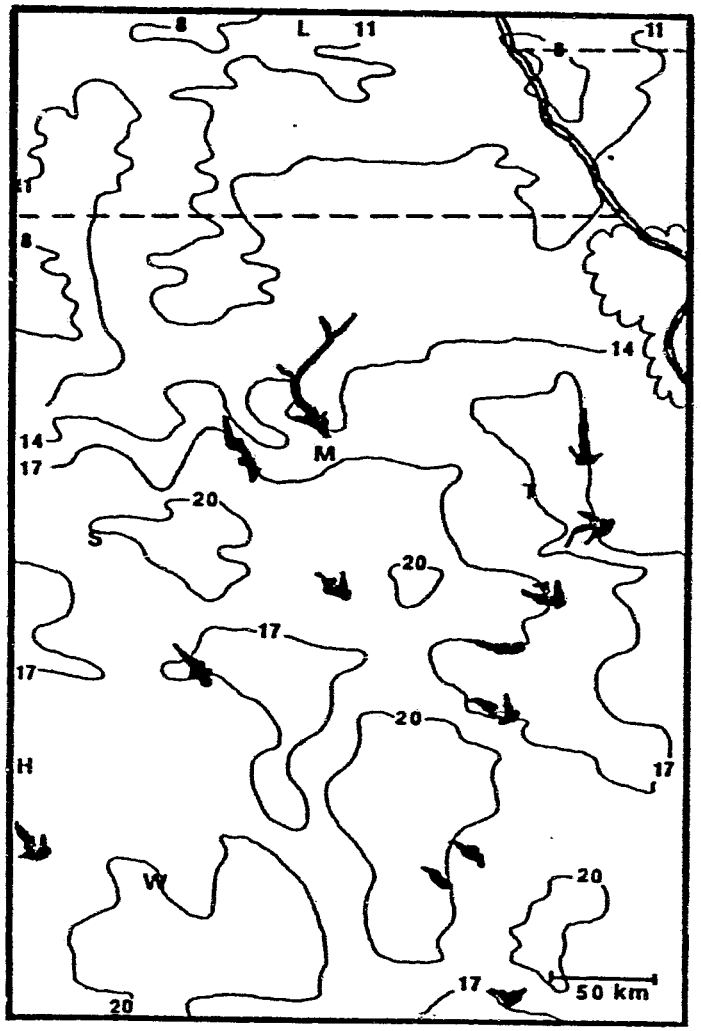

Figure 16. July 1, 1980 morning temperature rise (2000 - 1430 z).

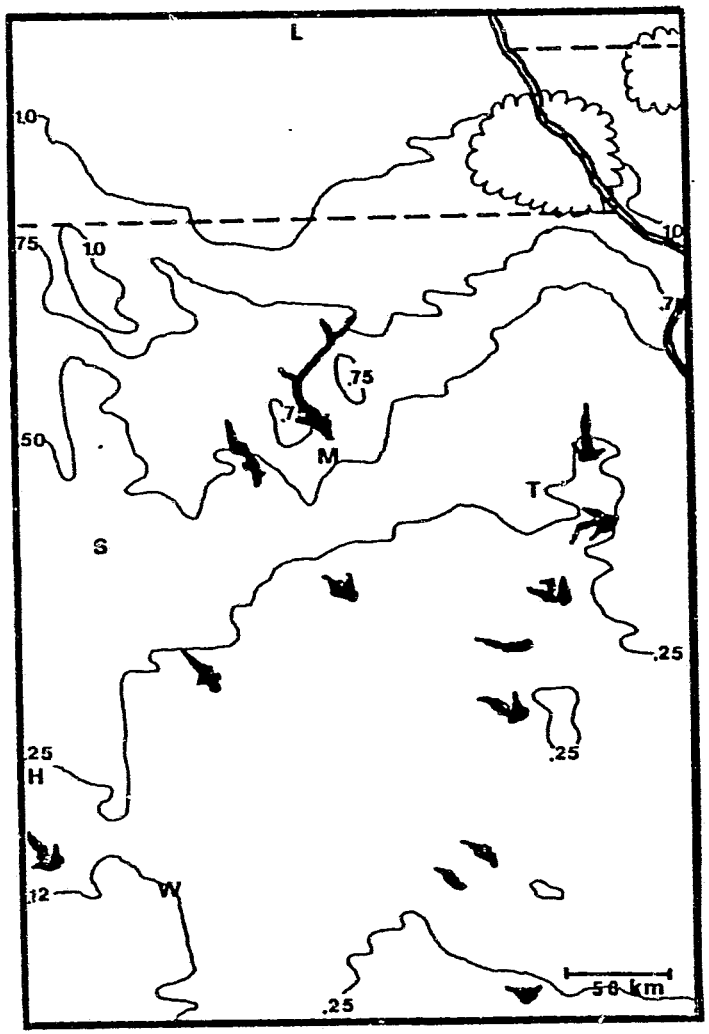

Figure 17. July 14, 1980 moisture availability.

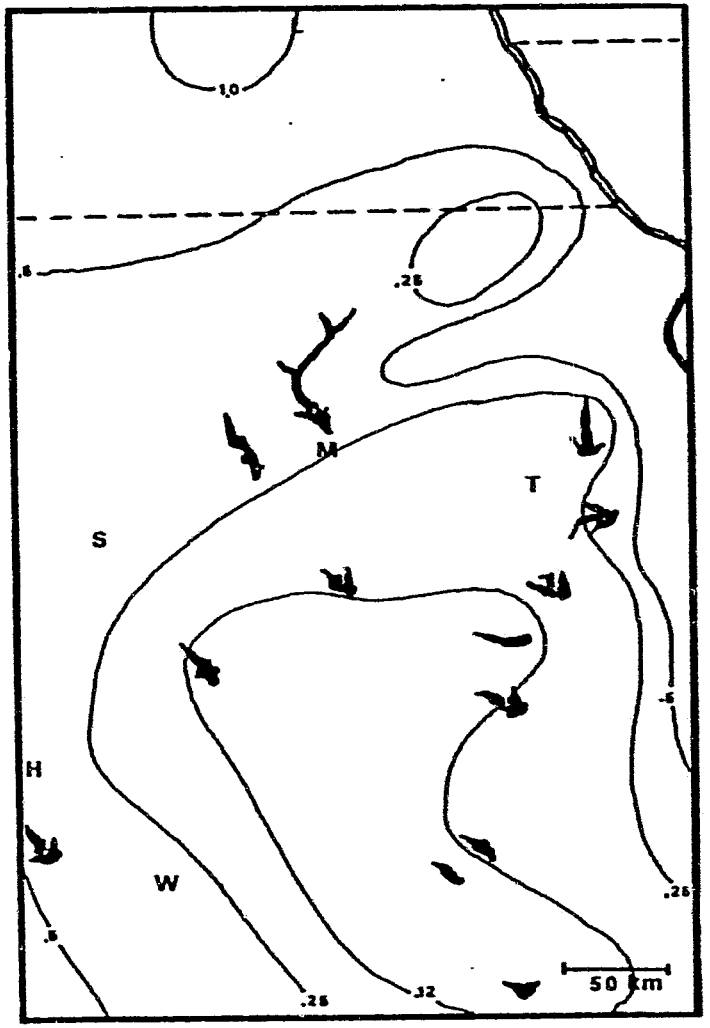

Figure 18. July 14, 1980 API analysis.

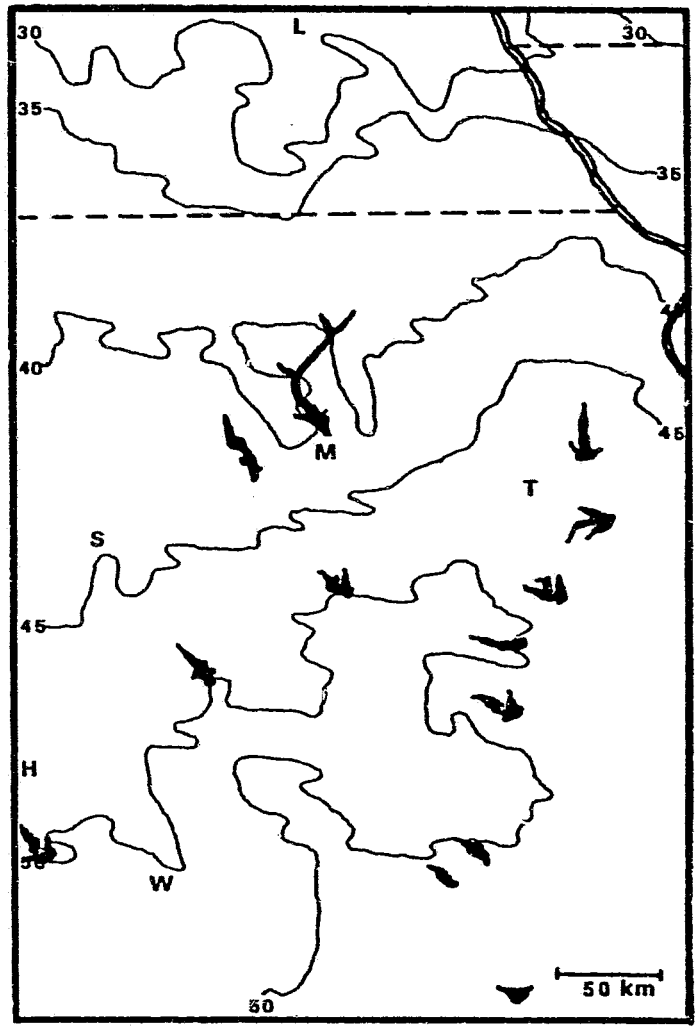

Figure 19. July 14, 1980 afternoon temperature (2000 z).

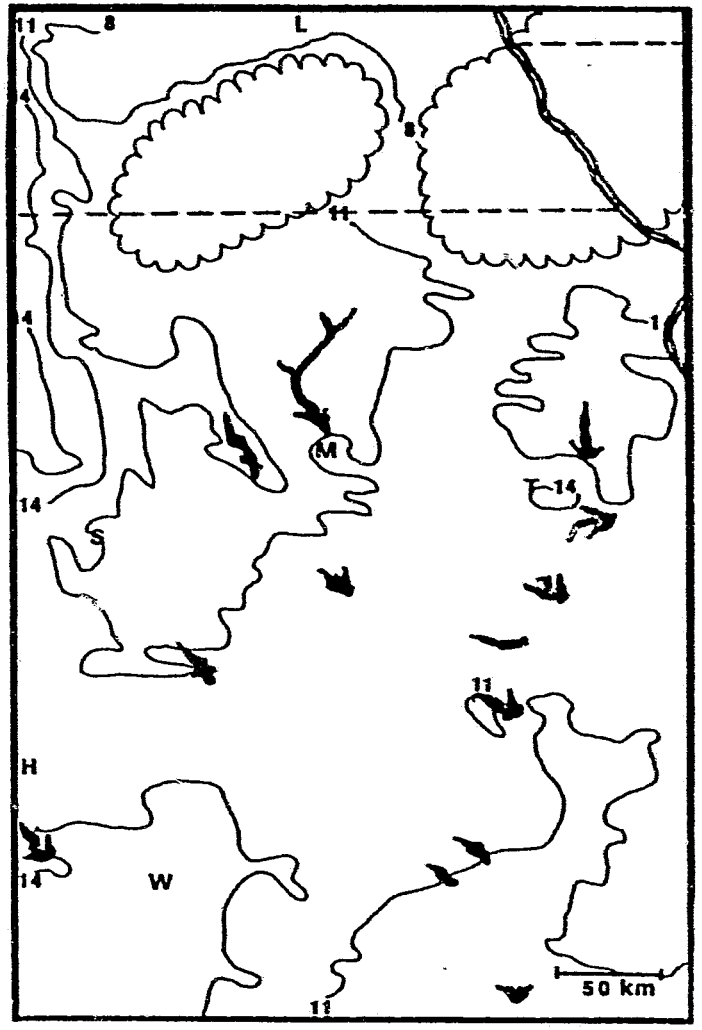

Figure 20. July 14, 1980 morning temperature rise (2000 - 1400 z).

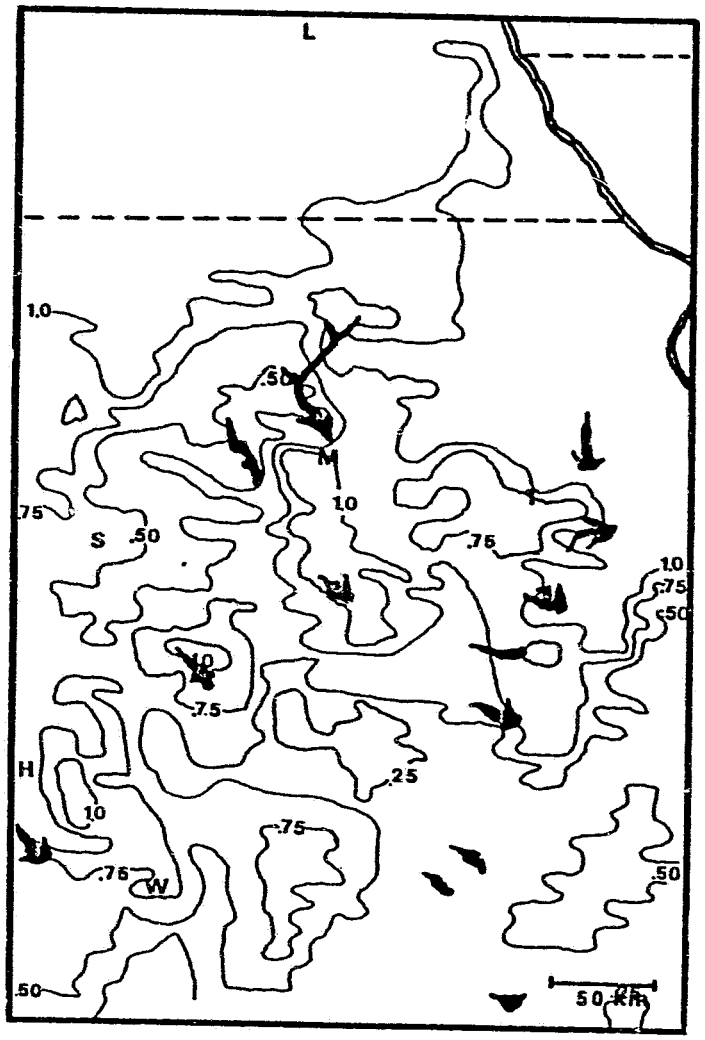

Figure 21. August 23, 1980 moisture availability.

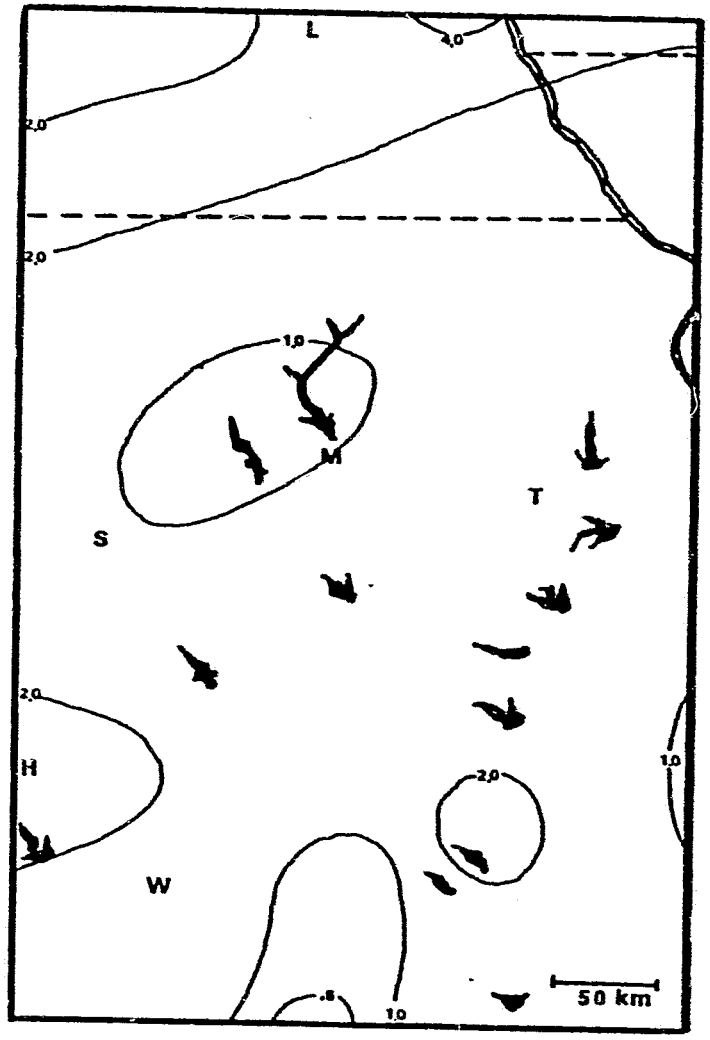

Figure 22. August 23, 1980 API analysis.

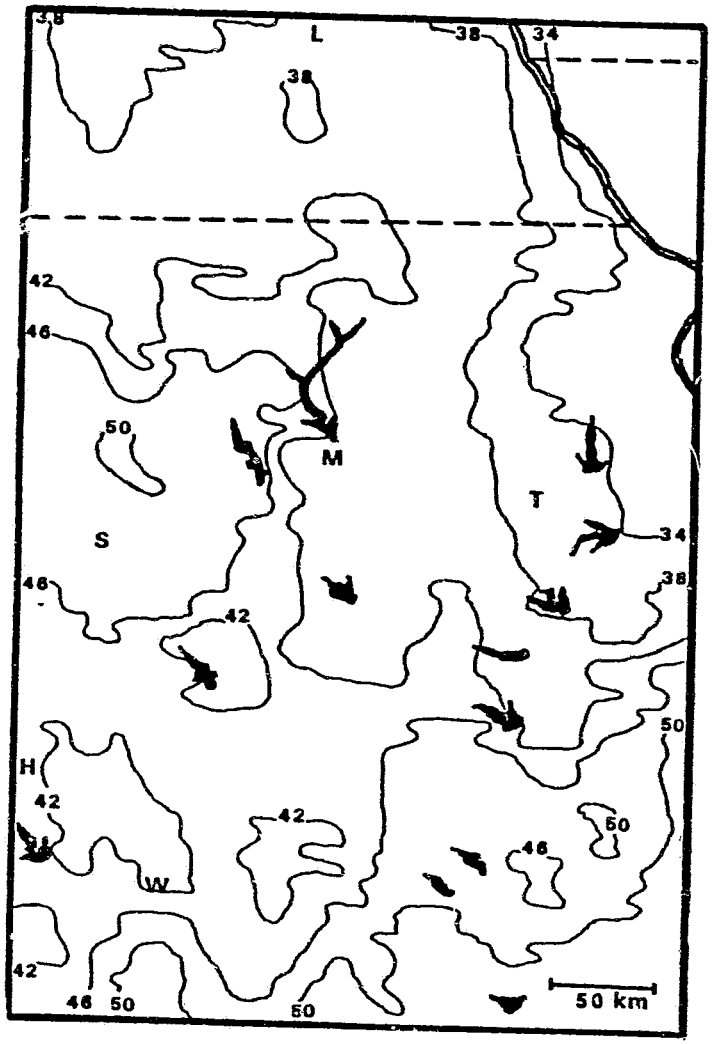

Figure 23. August 23, 1980 afternoon temperature (2000 z).

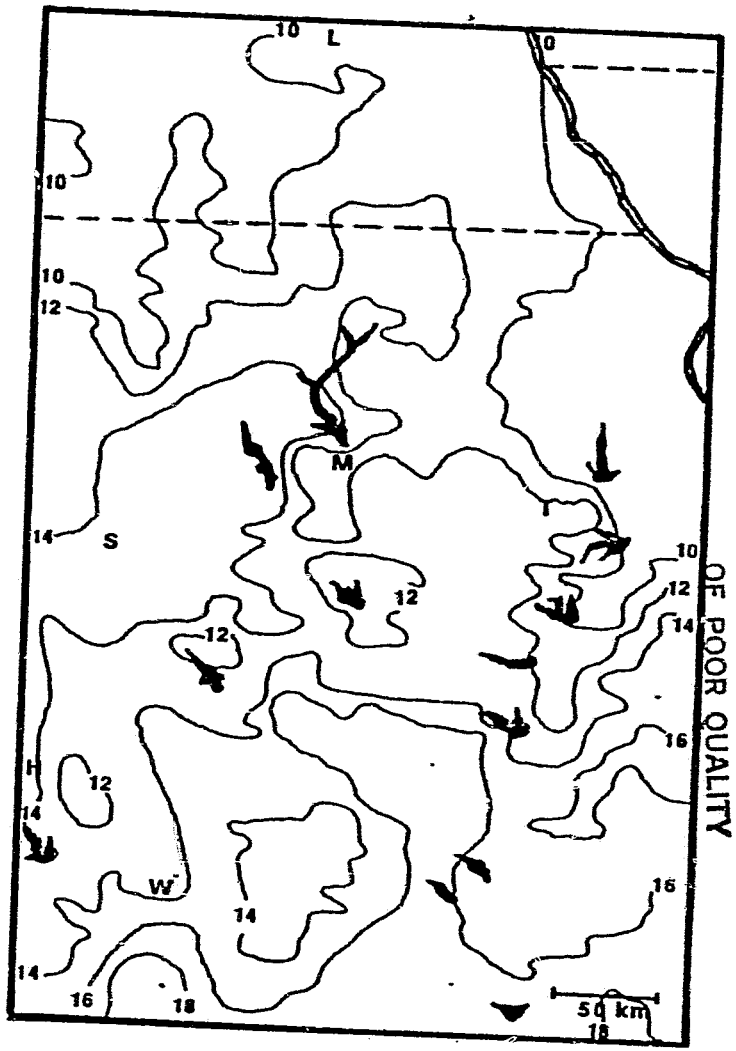

Figure 24. August 23, 1980 morning temperature rise 2000 – 1400 z).

10-12 kts from the southwest making this day adequate, but not ideal, for the inference of the soil moisture parameter. Areas of clouds were present to the northeast and south of Wichita in the morning (1430 Z) image. Although the meteorological conditions were not ideal for this day, a reasonably significant R^2 of 0.46 was obtained from the correlation of API and M.

It must also be pointed out that the drought situation was eased considerably by rainfall occurring during the early part of August. The API over the entire area increased significantly and became more uniform causing most of the data for correlation of API and M to be shifted to high values of each.

4.4 Cases Using the Day-Night Afternoon Technique

4.4.1 June 27, 1980

This case was analyzed using data from the afternoon (19 Z) image alone. The morning (1430Z) image was heavily contaminated by clouds. Both an analysis of M using the afternoon image alone and an analysis using the difference technique are presented in the subsequent figures. The correlation between M and API is performed only on the analysis using the afternoon temperature image.

Warm advection occurred during the day with surface winds from the southwest at 10-15 ks. Low humidities in the 20-30% range were present during the afternoon. The large and inherently gusty winds over the area no doubt influenced local variations in surface temperature causing a low R^2 of 0.37 to result.

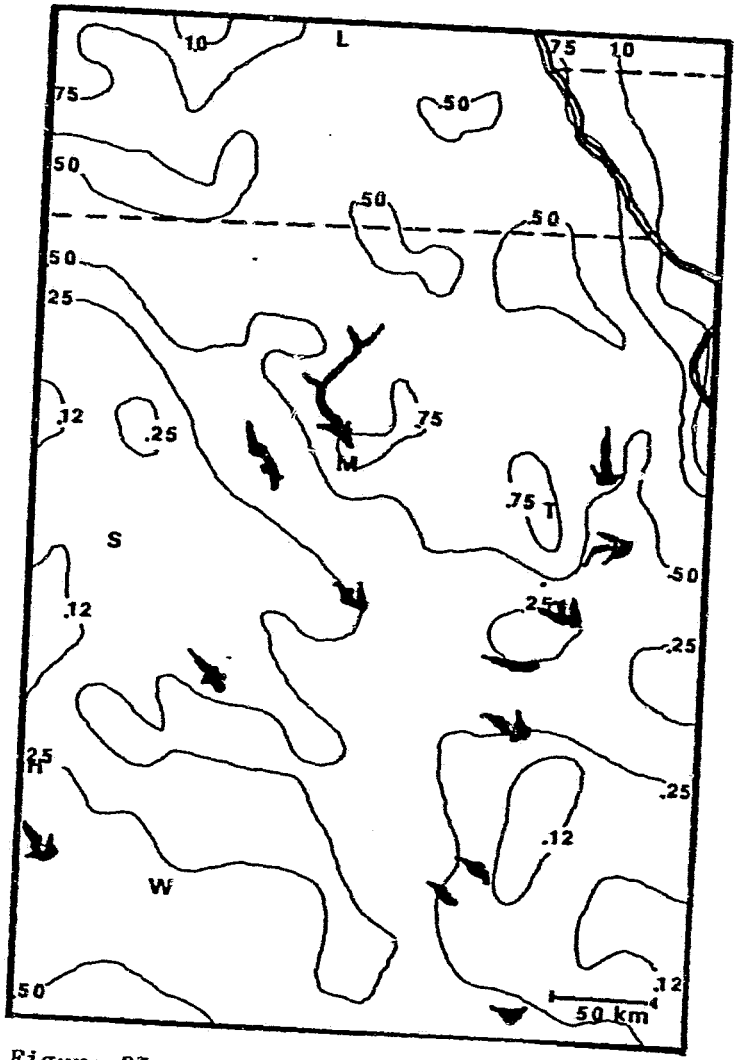

Figure 25. June 27, 1980 moisture availability taken from "afternoon" image technique.

Figure 26. June 27, 1980 API analysis.

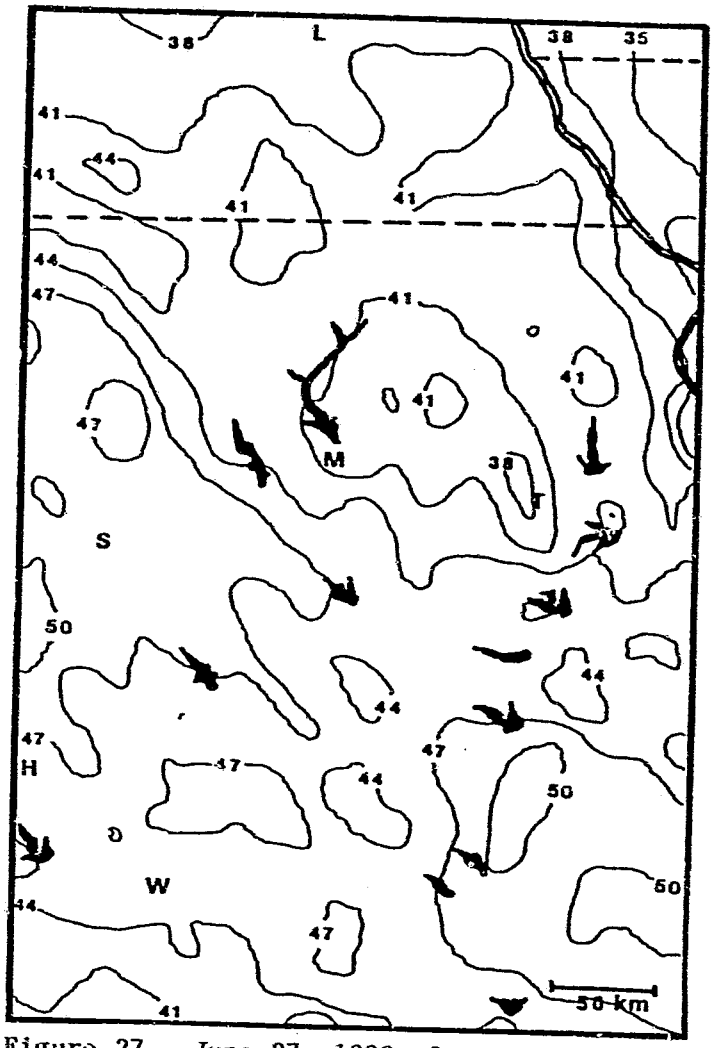

Figure 27. June 27, 1980 afternoon temperature (1900 z).

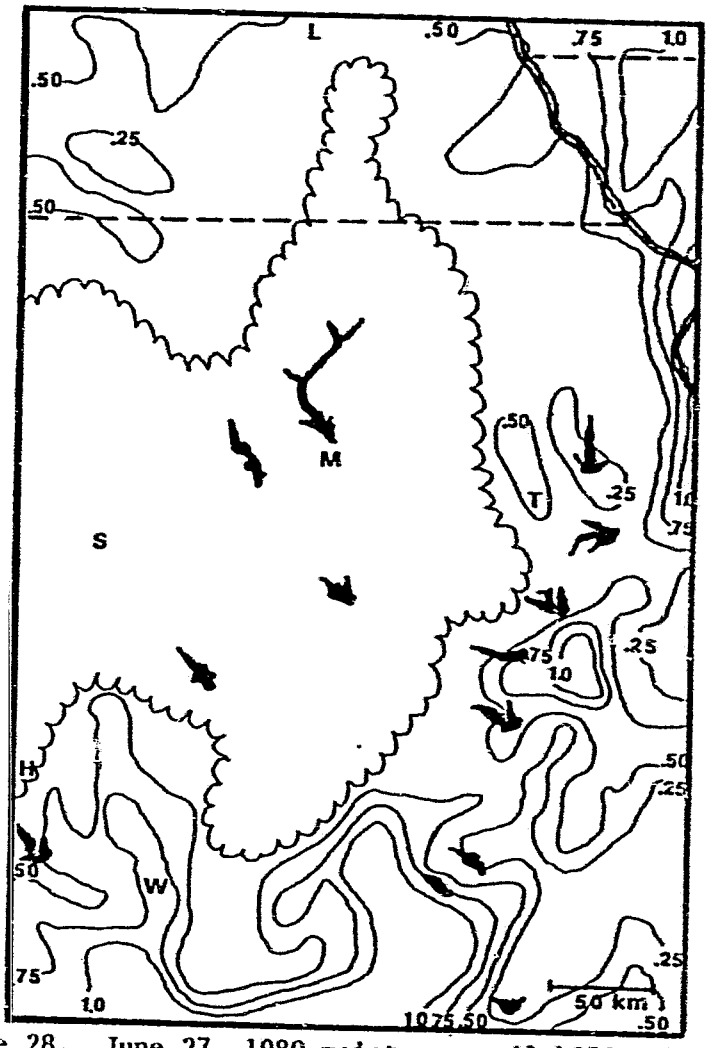

Figure 28. June 27, 1980 moisture availability by use of morning temperature rise technique.

4.2.2 June 30, 1980

In the June 30, 1980 case, which was analyzed using the "day-night" technique with a day image at 1900 Z (1300 local) and a night image at 0600 Z (2400 local), portions of the analysis were unusable because of clouds over Nebraska at the time of the night image. High humidities near 60% and strong southerly winds at 12-17 kts resulted in a poor sensitivity for the detection of moisture availability. An R^2 of 0.32 was found in the correlation of M and API.

4.4.3 July 6, 1980

The day-night two image technique with an afternoon time of 1930 Z and a night image time of 0600 Z are used for this case. Some clouds were present over the northwest corner of the night image. Moderate southwesterly winds at 8-12 kts with rather low humidities in the 30-50% range were present over the study area at the time of the afternoon (1930 Z) image. These conditions helped to attain a resulting R^2 of 0.51.

4.4.4 July 13, 1980

The analysis of this case used the day-night technique with an afternoon image at 20 Z and a night image at 06 Z. The raw data in the afternoon image showed a band of noisy values across the scene. The night image has clouds obscuring almost all of Nebraska and some portions of northern Kansas.

Weather conditions were marked by a very strong wind out of the south at 20 kts. The humidity over the area was very low with values

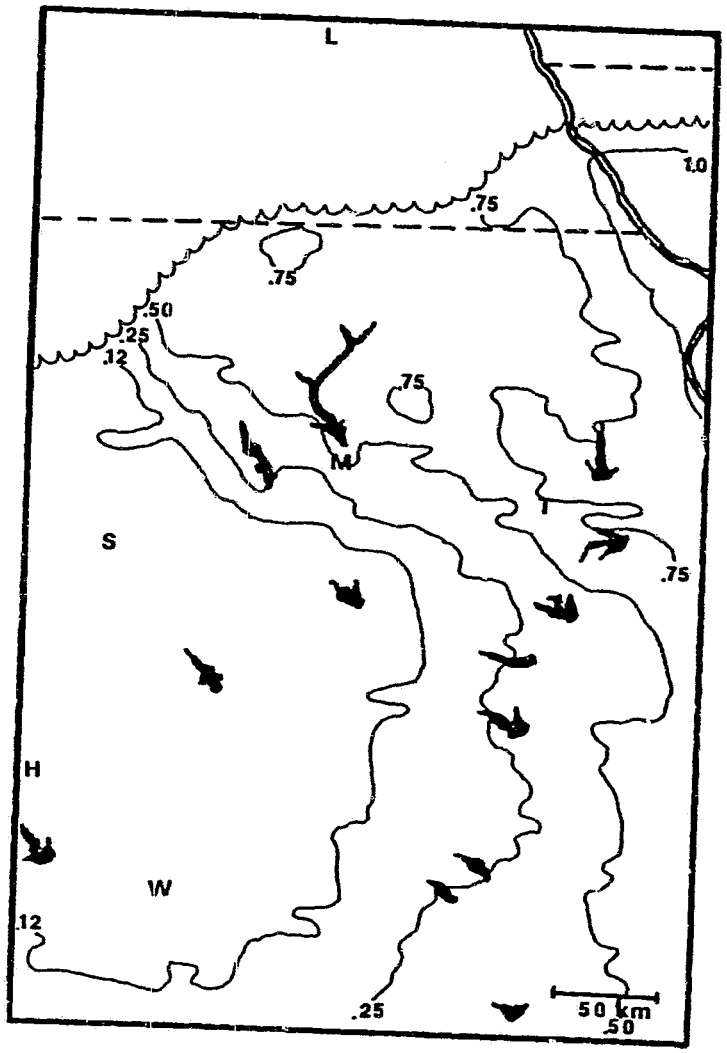

Figure 29. June 30, 1980 moisture availability using Day-Night" technique.

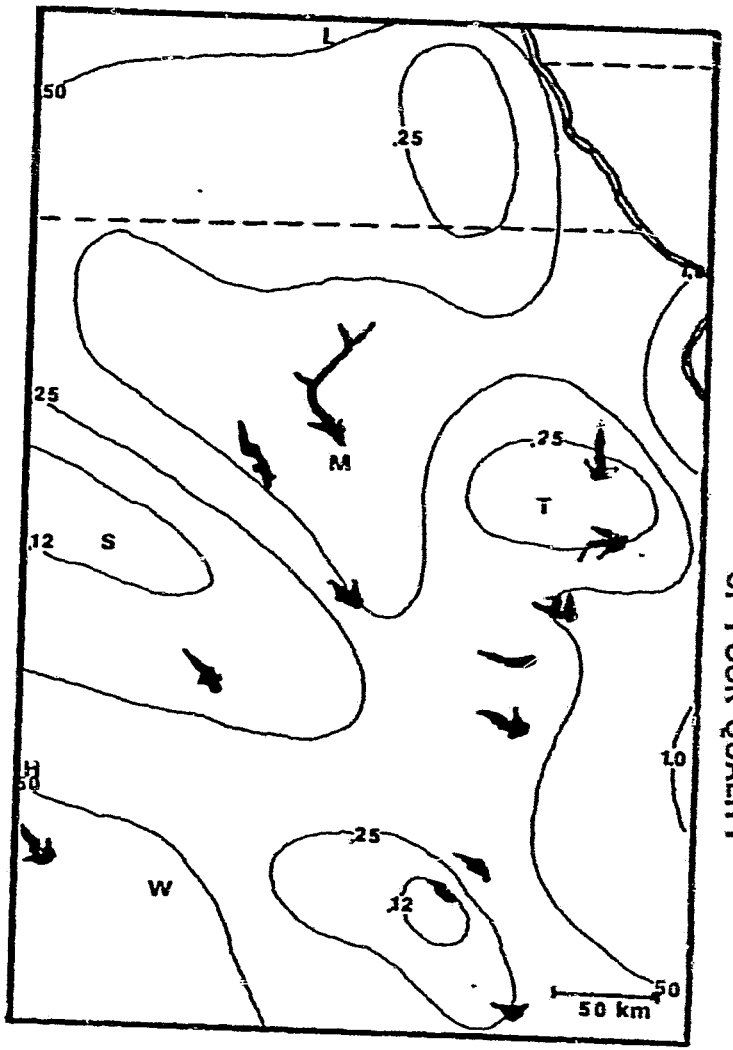

Figure 30. June 30, 1980 API analysis.

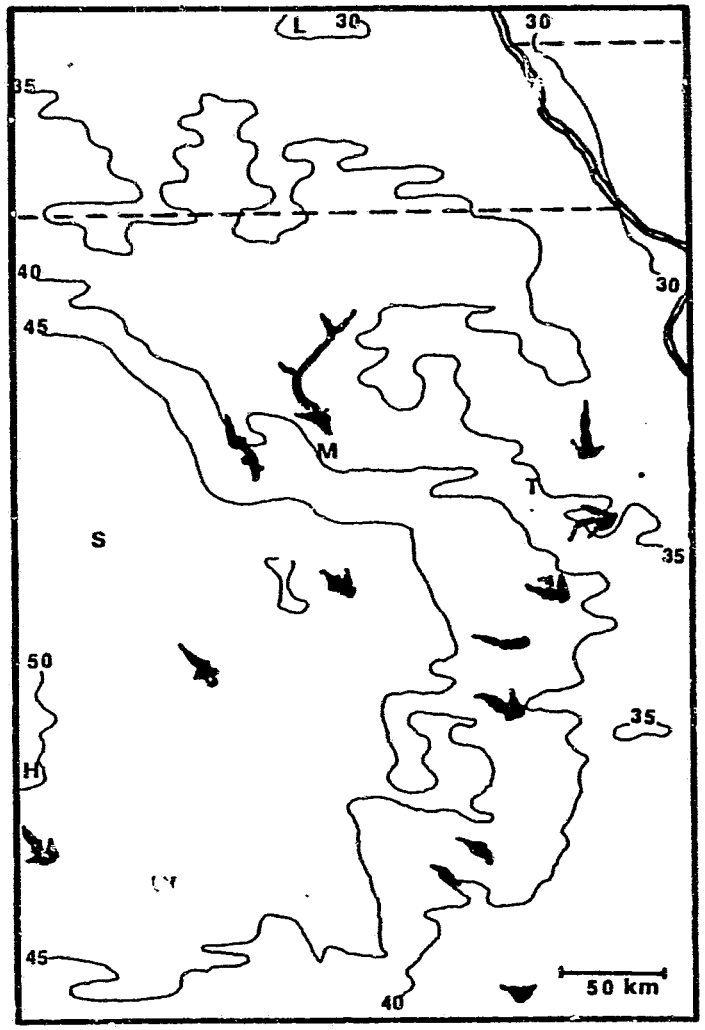

Figure 31. June 30, 1980 day temperature image (1900 z).

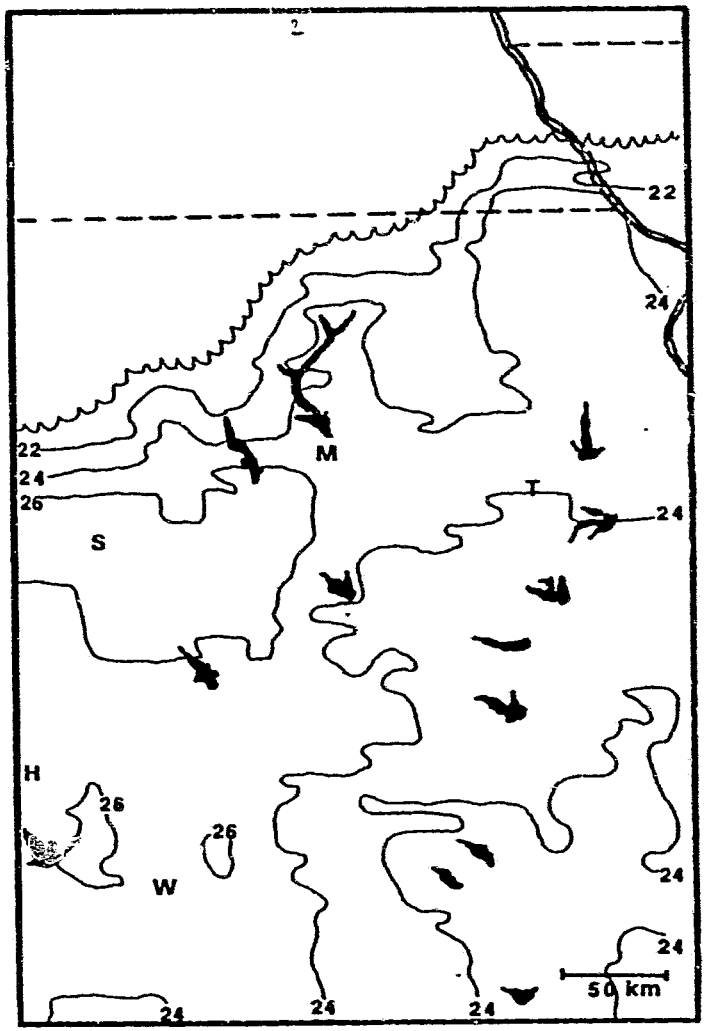

Figure 32. June 30, 1980 night temperature image (0609 z).

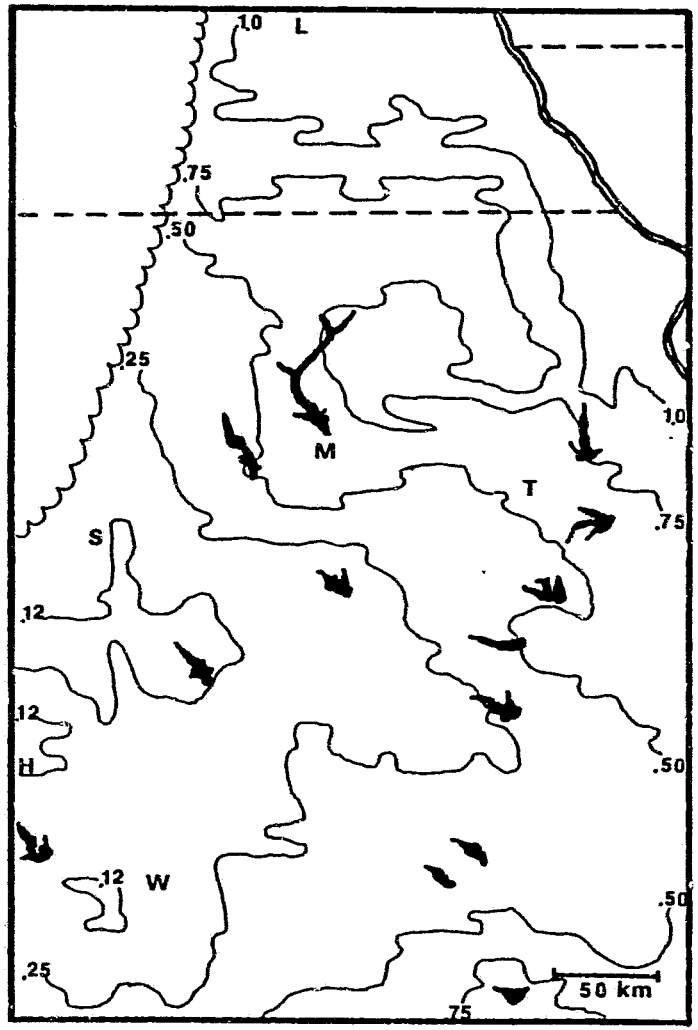

Figure 33. July 6, 1980 moisture availability using "Day-Night" technique.

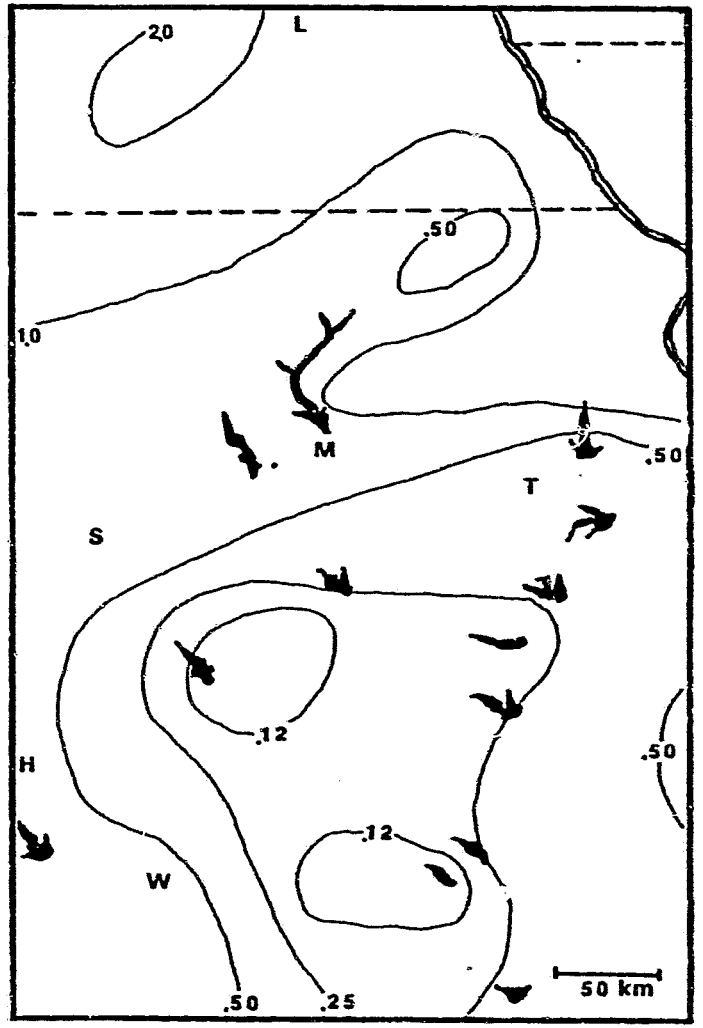

Figure 34. July 6, 1980 API analysis.

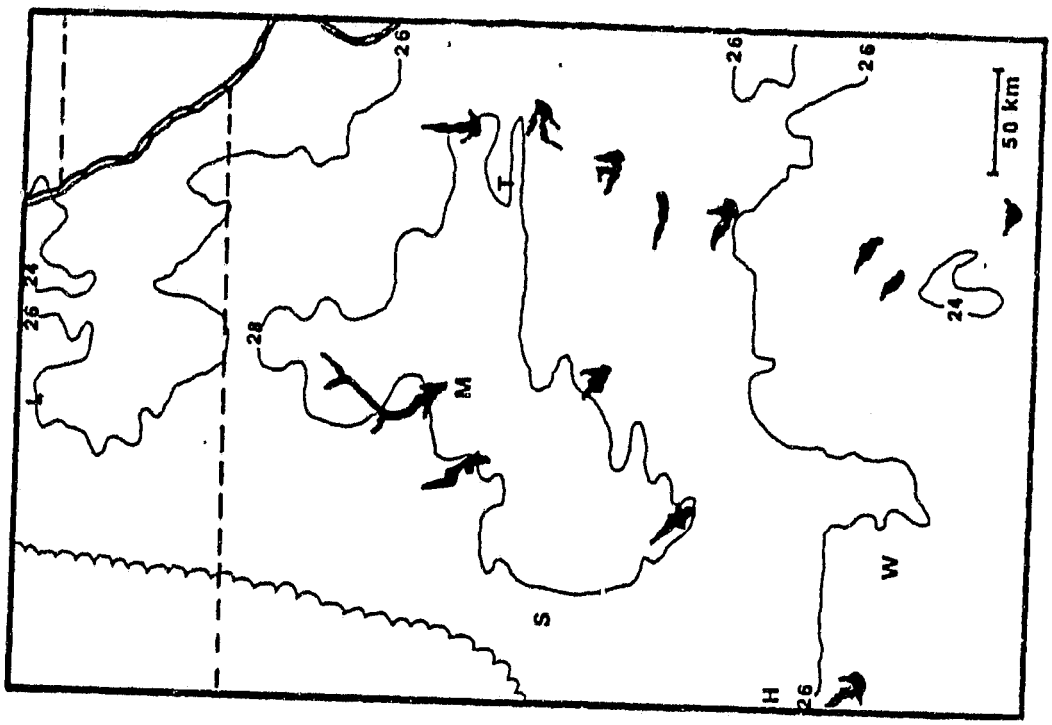

Figure 36. July 6, 1980 night temperature image (0600 z).

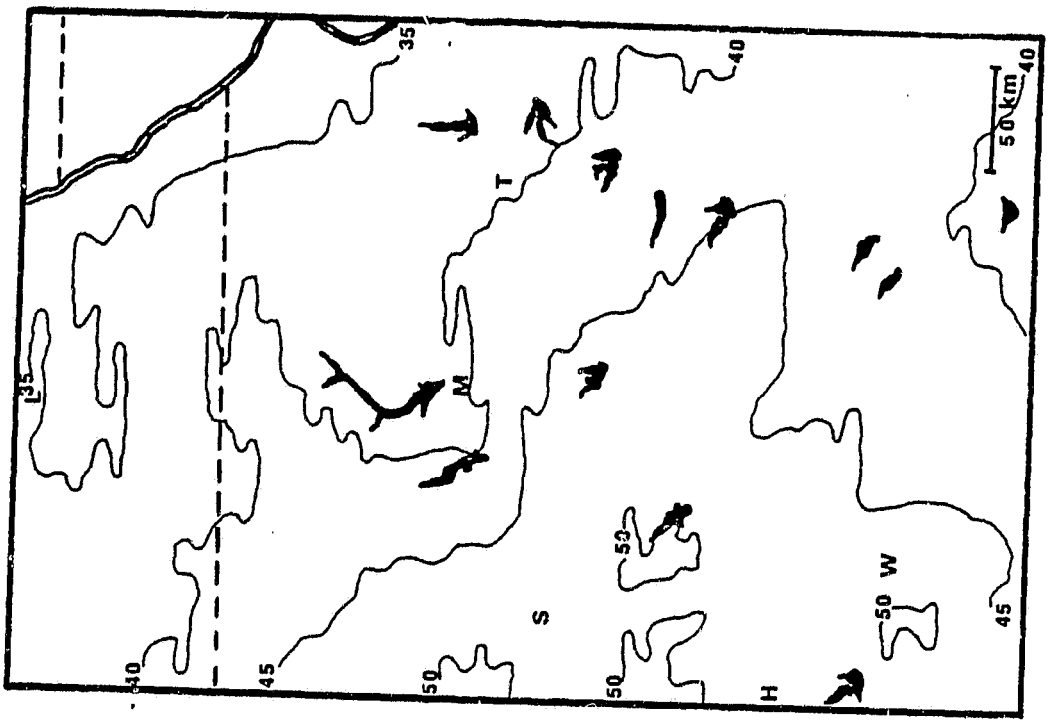

Figure 35. July 6, 1980 day temperature image (1930 z).

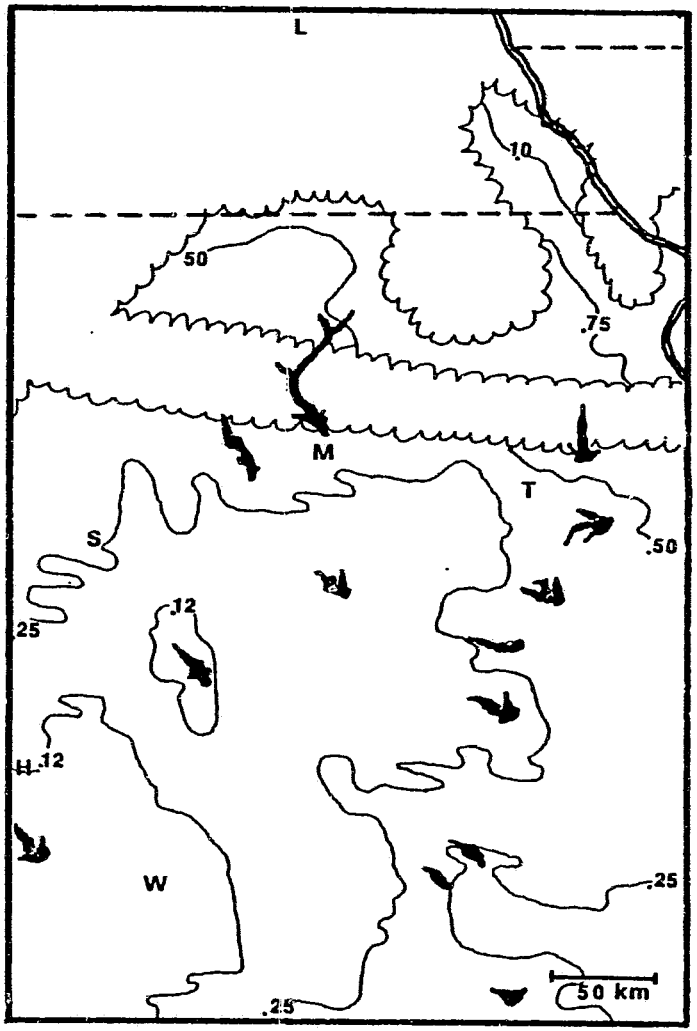

Figure 37. July 13, 1980 moisture availability using "Day-Night" techinque.

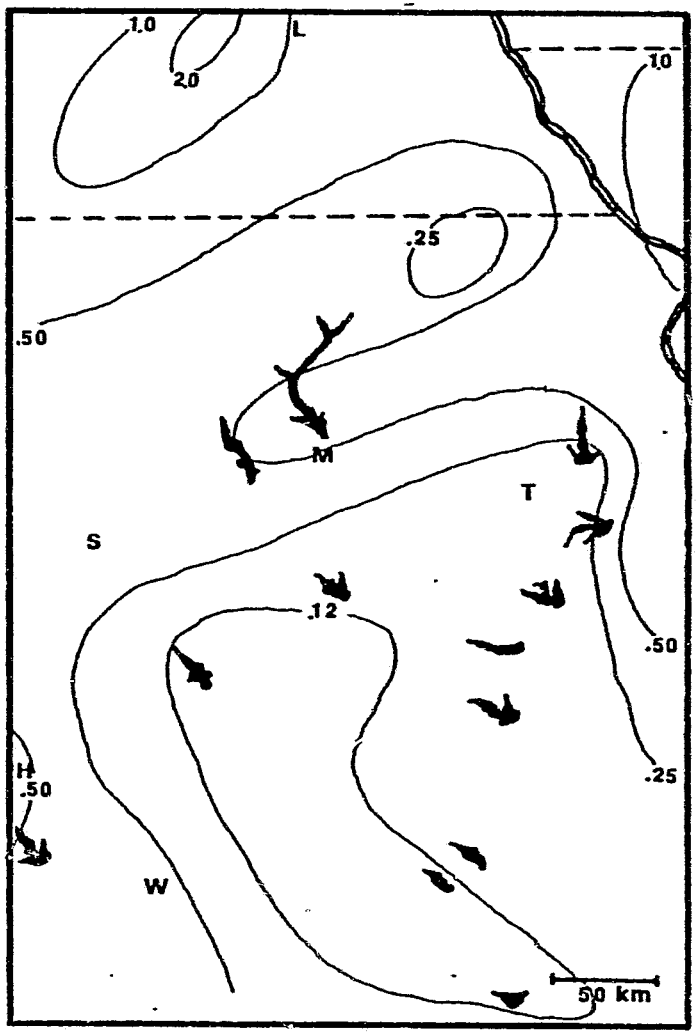

Figure 38. July 13, 1980 API analysis.

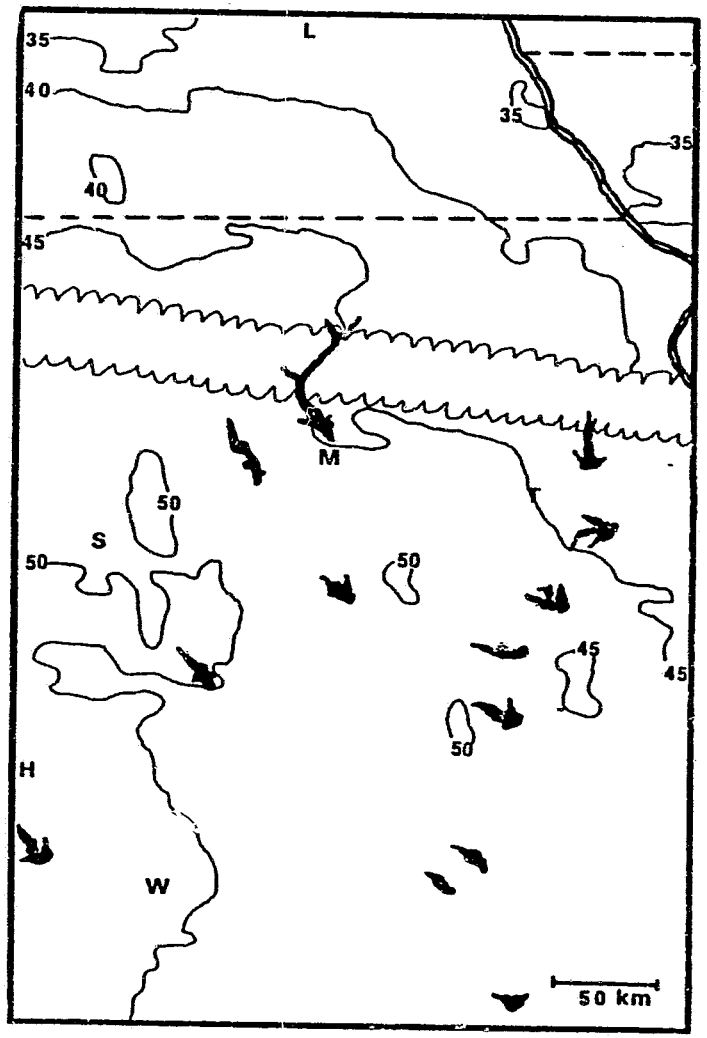

Figure 39. July 13, 1980 day temperature image (2000 z).

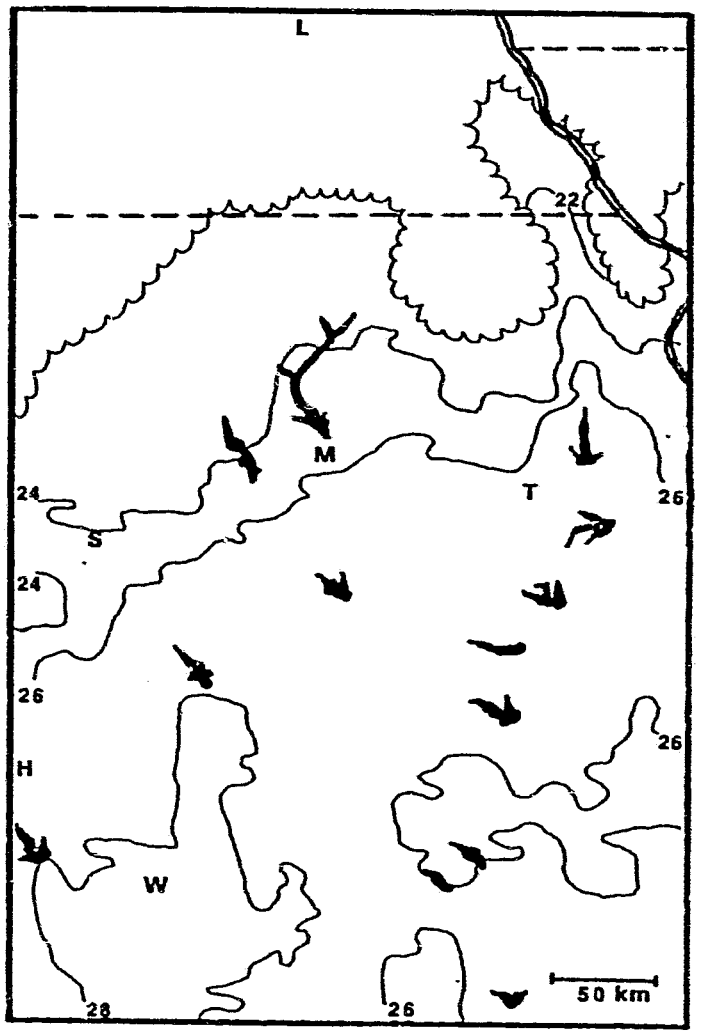

Figure 40. July 13, 1980 night temperature image (0600 z).

of 20-30%. The strong winds present contributed to the relatively small amplitude of surface temperature variations over the area, causing a reduced accuracy in the determination of soil moisture. An R^2 value of 0.41 was obtained for this case.

4.4.5 July 22, 1980

Weather conditions for this day were nearly ideal for the inference of soil moisture within the study area. Clouds were not present in any of the afternoon (20 Z) image and only a small area in the northwest corner of the nighttime (06 Z) image was obscured.

The region was covered by a large high pressure system, centered in Nebraska, which kept winds light and variable at less than 5 kts during the entire day. In addition to the light winds, low humidities near 20% helped to give the surface temperature response a large sensitivity to conditions, a very good correlation between M and API resulted. The R^2 value otained was 0.74.

4.4.6 July 28, 1980

A light southwesterly breeze at 5-8 kts dominated the study area during most of the day as a weak low pressure trough approach the area. Some clouds were present in the southern quarter of the afternoon (19 Z) image. Humidity was low, in the 30-40% range, at this time. The light winds and low humidity helped to enhance the temperature variation, due to soil moisture differences, over the usable cloud-free area resulting in a large R^2 of 0.74.

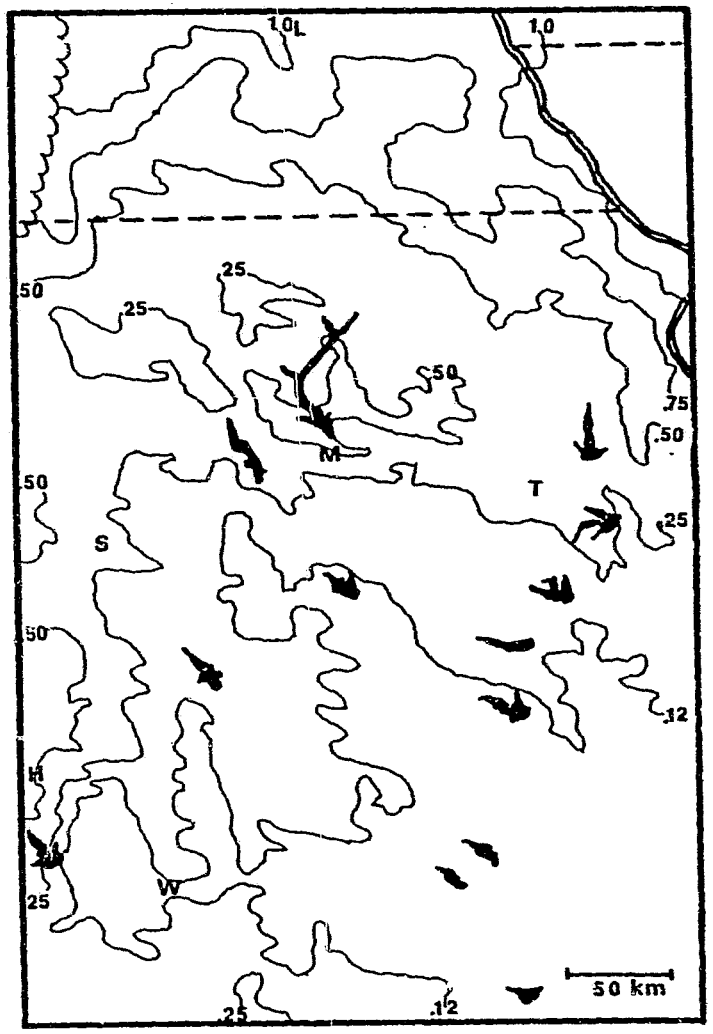

Figure 41. July 22, 1980 moisture availability using "Day-Night" technique.

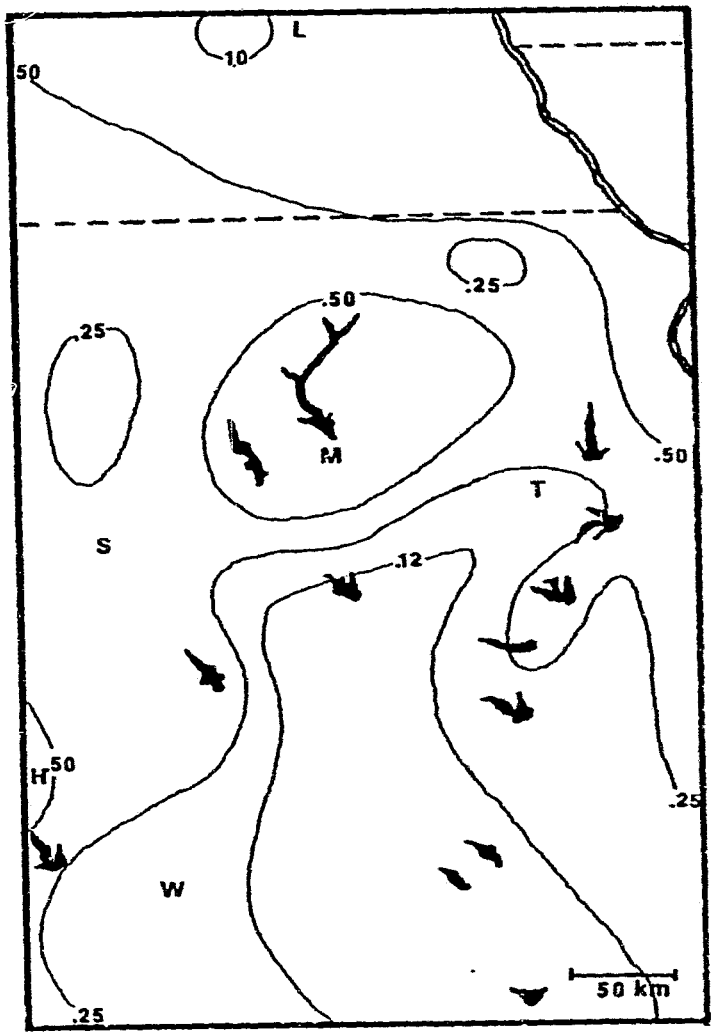

Figure 42. July 22, 1980 API analysis.

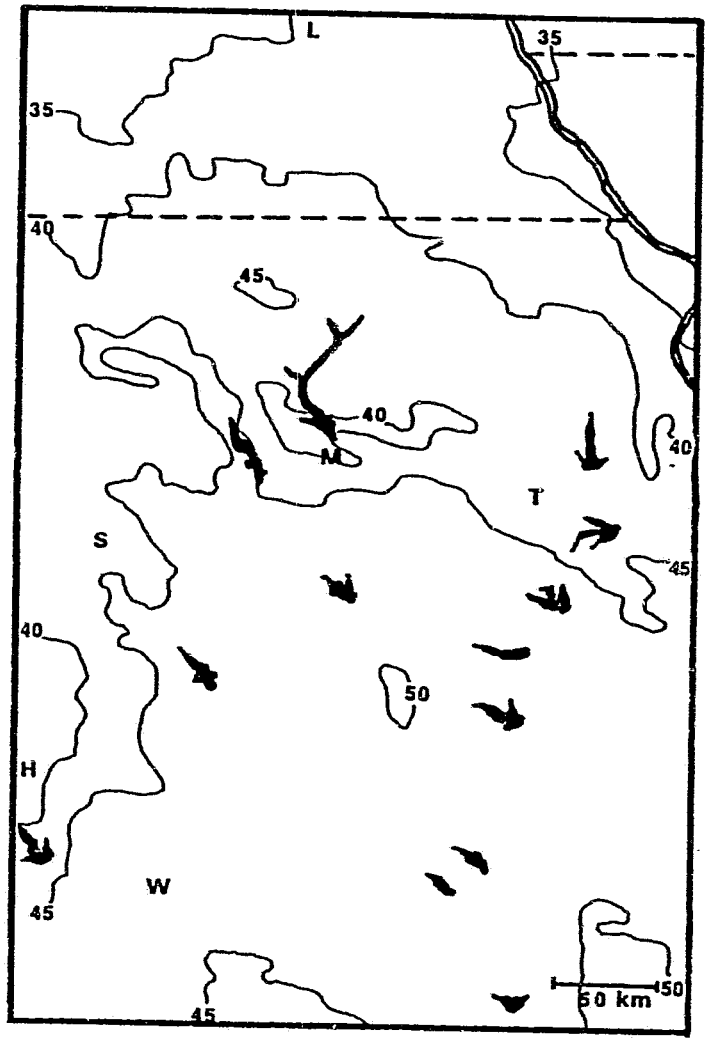

Figure 43. July 22, 1980 day temperature image (2000 z).

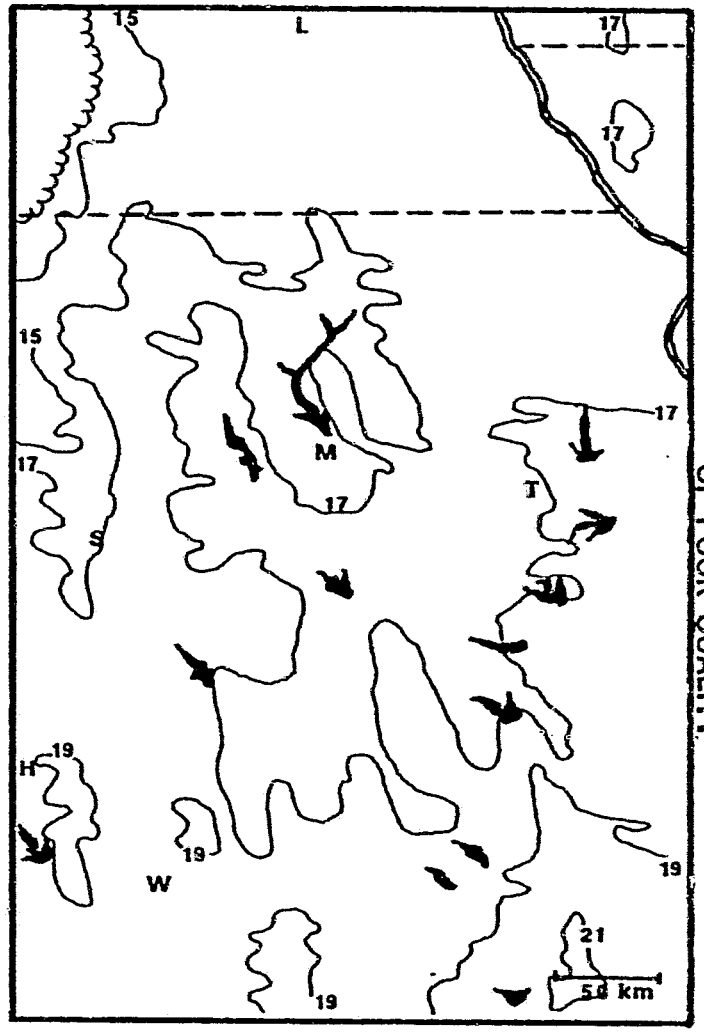

Figure 44. July 22, 1980 night temperature image (0600 z).

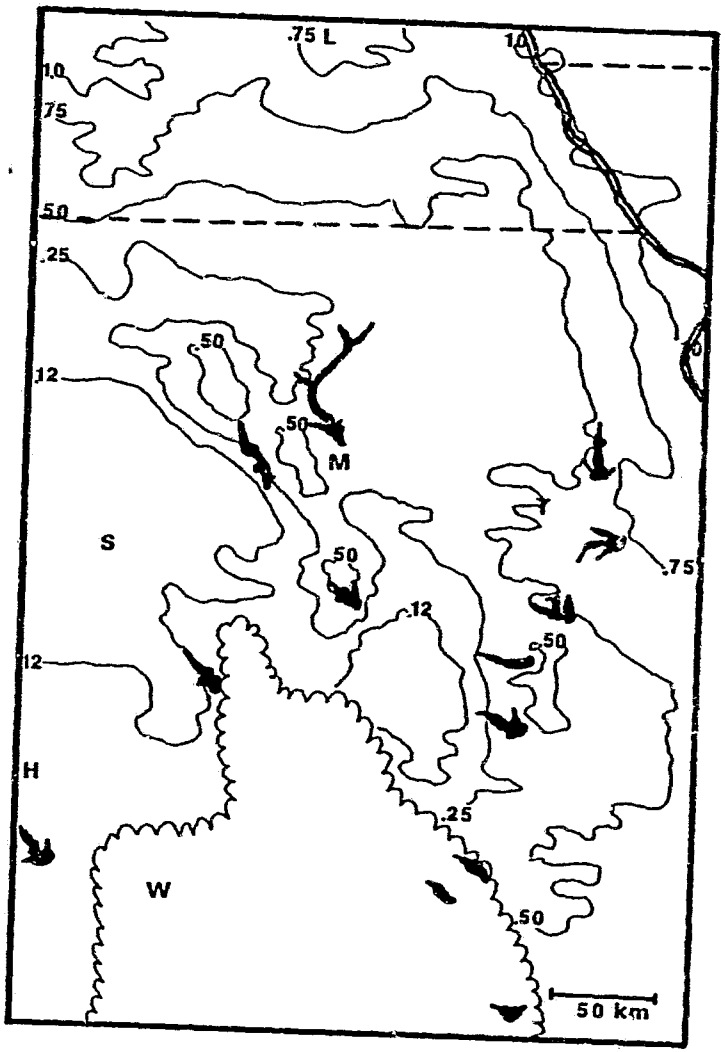

Figure 45. July 28, 1980 moisture availability using "Day-Night" technique.

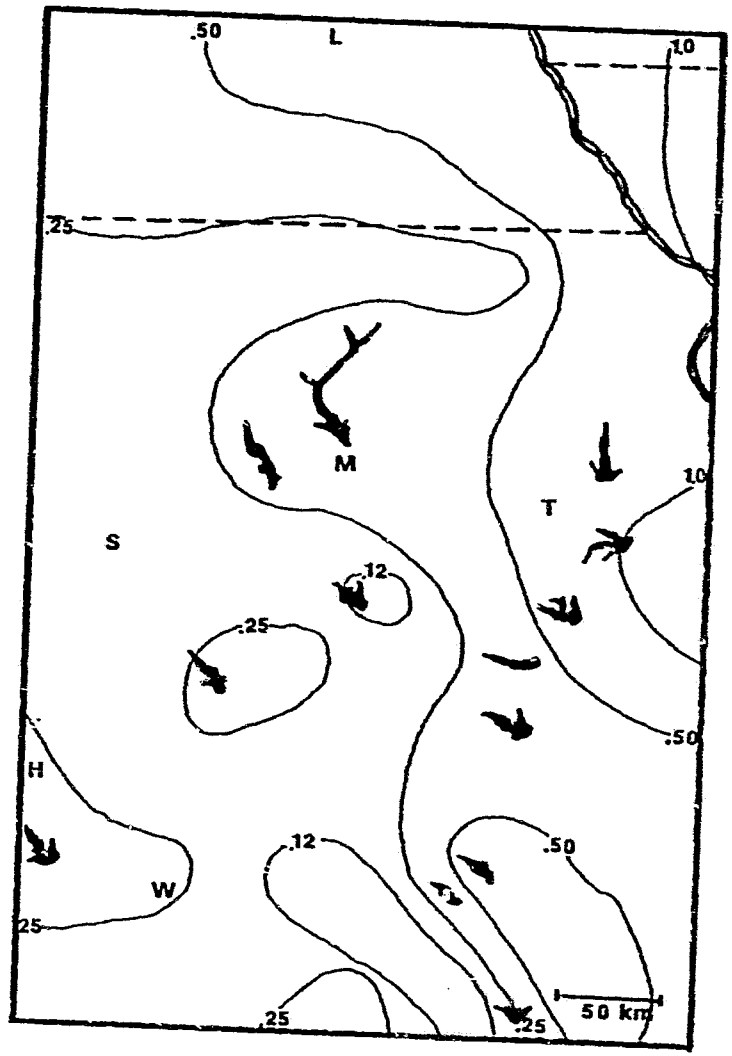

Figure 46. July 28, 1980 API analysis.

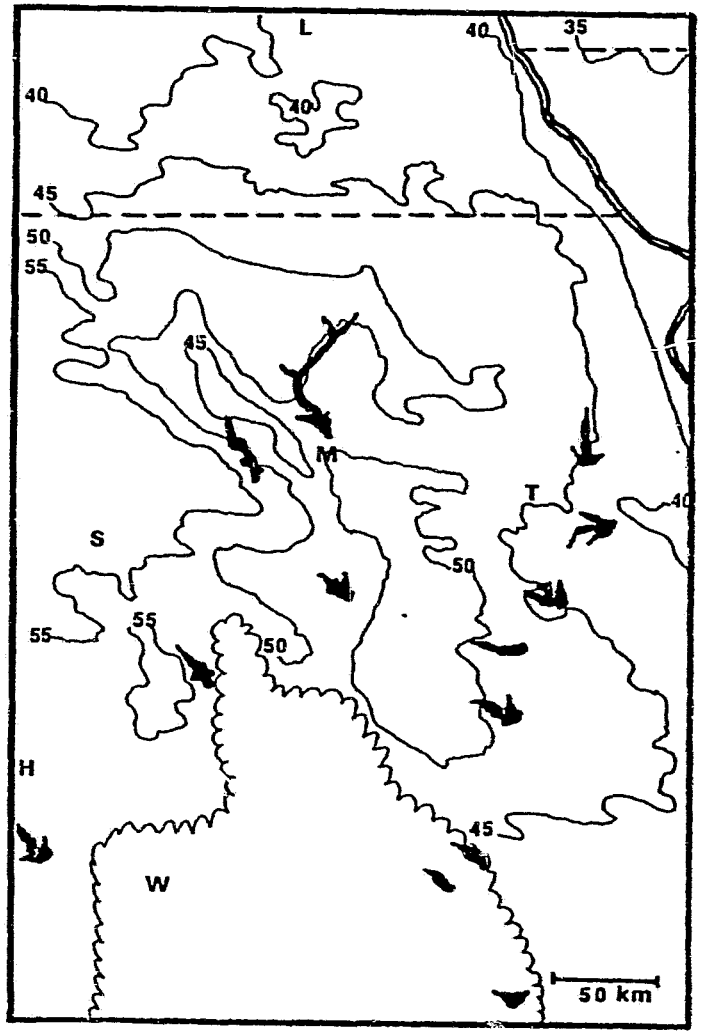

Figure 47. July 28, 1980 day temperature image (2000 z).

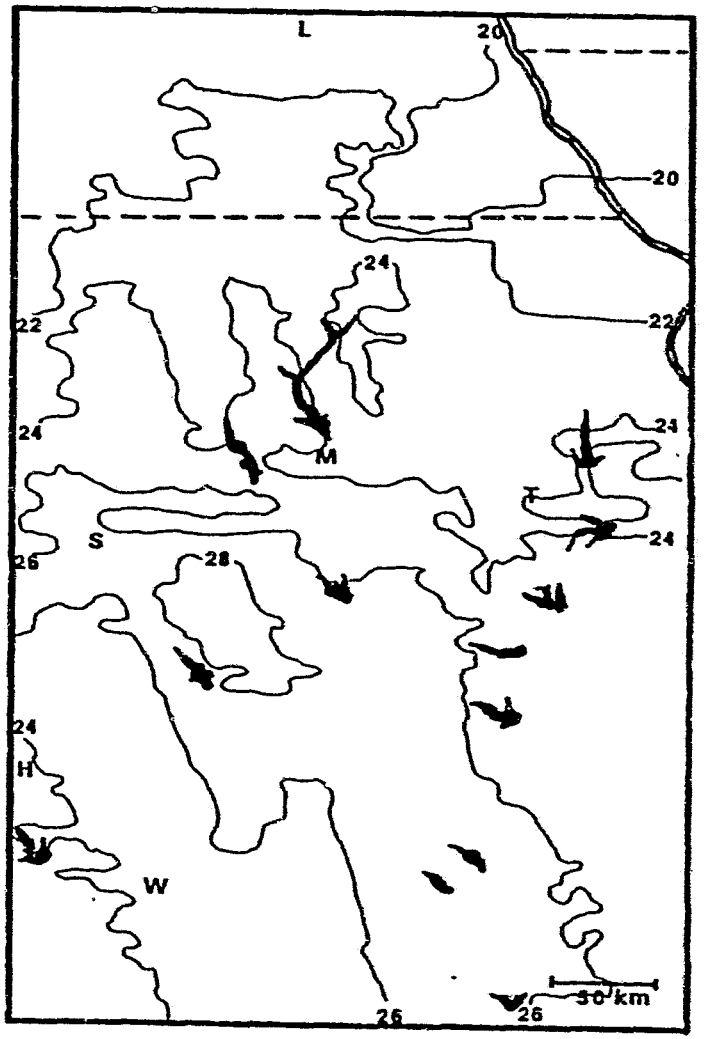

Figure 48. July 28, 1980 night temperature image (0600 z).

4.4.7 July 29, 1980

This case was originally chosen to be analyzed using the morning temperature rise technique but the presence of clouds in the morning (1430 Z) image necessitated the use of the single afternoon image technique. An analysis of M is generated using the morning temperature rise technique but, as can be seen in the figures, it is loaded with clouds and even the unscalloped (cloud free) portion may be influenced by "noise" from morning clouds.

The clouds in the morning image were caused by the passage of the low pressure trough that approached the area on July 28 (previous case). By afternoon, after the passage of the trough, winds became south to southeast at 8-12 kts with humidities in the 20-30% range. In spite of the presence of clouds in the morning the analysis of M using the single afternoon image technique brought an R^2 of 0.55 in the correlation of M and API.

4.5 Summary of Results

Two basic techniques have been presented as a means of inferring soil moisture. The morning temperature rise technique and results from the day-night technique and the one afternoon image technique. The latter two techniques are combined into one category because the afternoon (day) image contains nearly all of the information concerning soil moisture. The value of the night image in the day-night technique is used in obtaining an estimate of thermal inertia (see Dodd, 1979).

Table 1 gives a summary of the regression statistics from the cases using the morning temperature rise technique. Table 2 give a

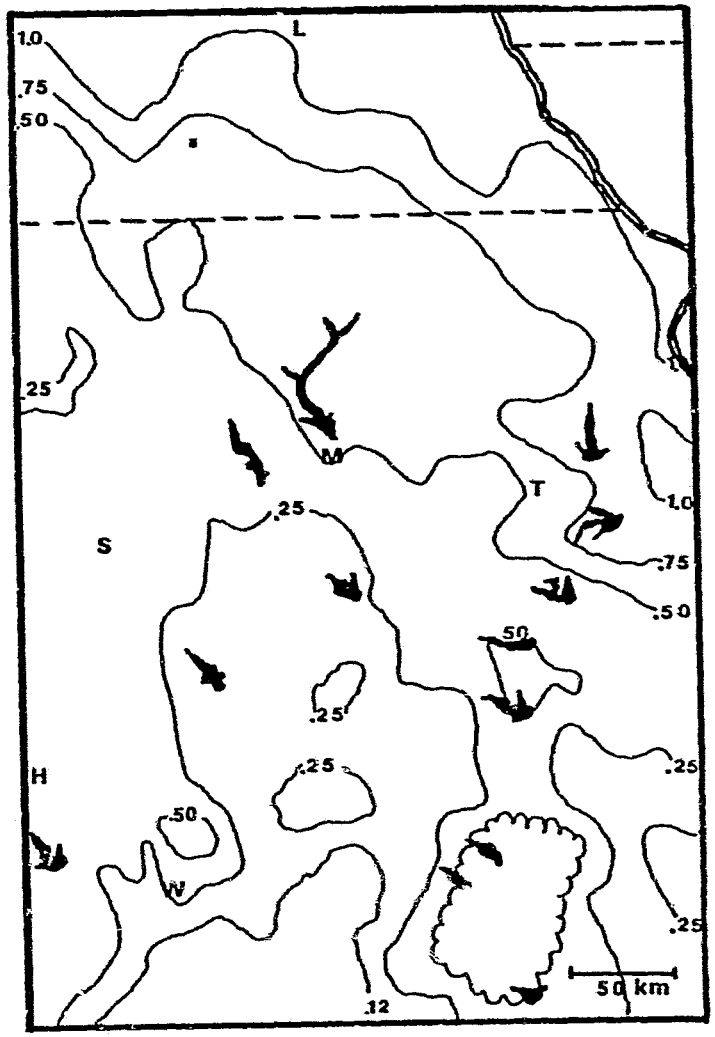

Figure 49. July 29, 1980 moisture availability using "Afternoon Image" technique.

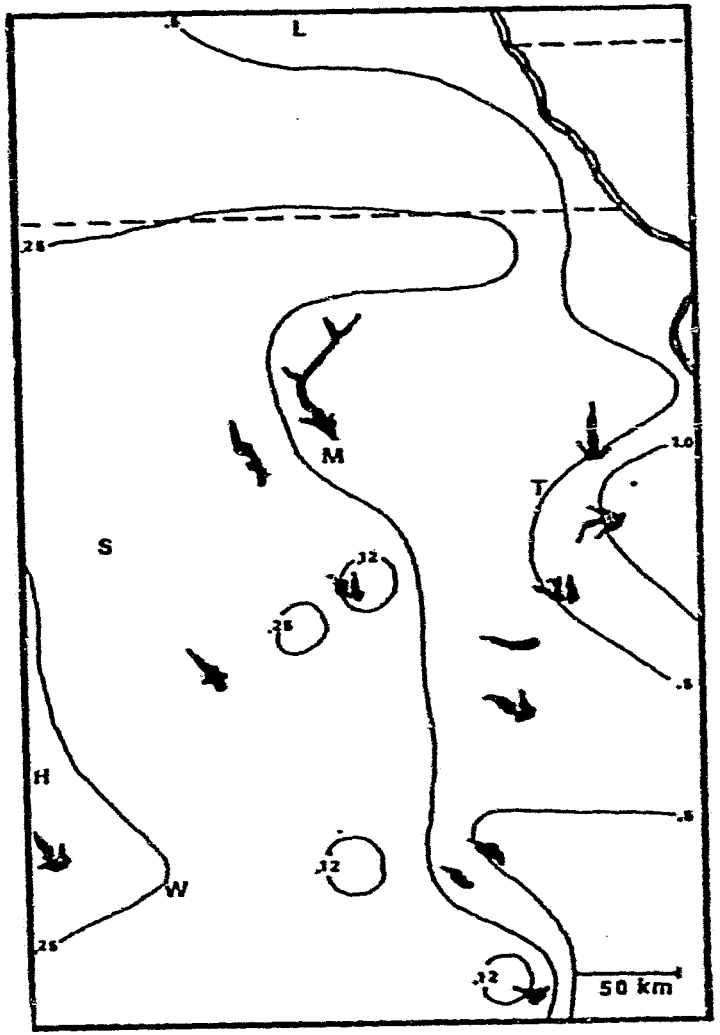

Figure 50. July 29, 1980 API analysis.

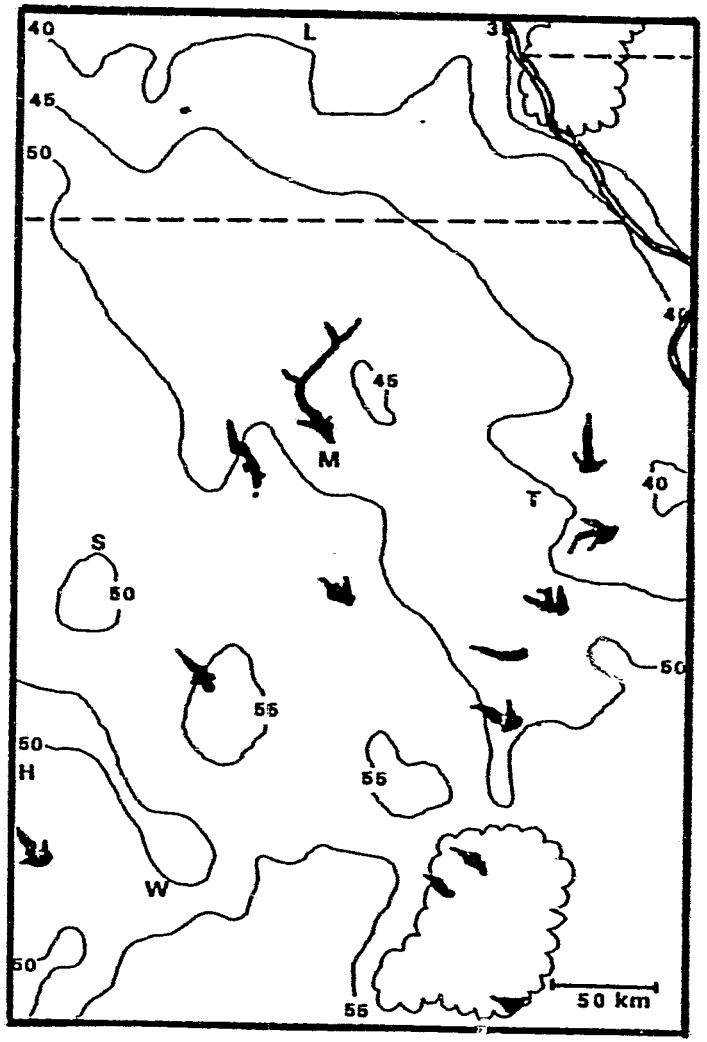

Figure 51. July 29, 1980 afternoon image (2000 z).

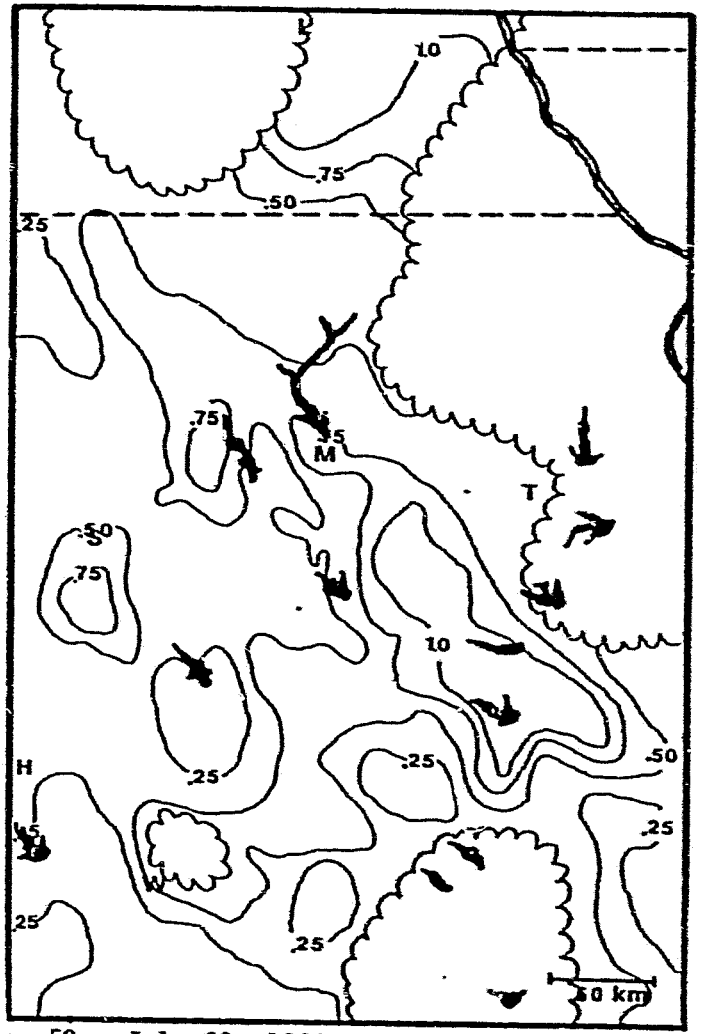

Figure 52. July 29, 1980 moisture availability using "morning temperature rise" technique.

TABLE 1

Summary of Regression Statistics for Cases Using the "Morning Temperature Rise" technique

Case	Date	Regression Equation	Standard Deviation Intercept	Standard Deviation Slope	T-Ratio Slope	R^2%	Number of Points	% of Image Clear
a	July 15, 1978	Log API = 1.47 + 2.57 M	.146	.189	13.6	73.0	69	66
b	July 27, 1978	Log API = 0.87 + 2.79 M	.304	.381	7.3	38.7	84	81
c	July 1, 1980	Log API = 1.42 + 0.47 M	.105	.214	2.21	4.6	82	79
d	July 14, 1980	Log API = 0.11 + 2.54 M	.127	.215	11.82	63.1	82	79
e	Aug 23, 1980	Log API = 2.42 + 1.40 M	.134	.169	8.3	46.4	80	77

TABLE 2

Summary of regression statistics for cases using the "Day-Night" Technique

Case	Date	Regression Equation	Standard Deviation Intercept	Standard Deviation Slope	T-Ratio Slope	R^2%	Number of Points	% of Image Clear
f	June 27, 1980	Log API = 1.23 + 2.03 M	.148	.283	7.15	37.6	84	81
g	June 30, 1980	Log API = 1.14 + 1.61 M	.122	.252	6.38	31.9	86	83
h	July 6, 1980	Log API = .737 + 2.55 M	.155	.259	9.87	50.6	95	91
i	July 13, 1980	Log API = .075 + 3.07 M	.154	.423	7.27	40.9	76	73
j	July 22, 1980	Log API = .10 + 2.88 M	.081	.170	16.9	74.3	100	96
k	July 28, 1980	Log API = .52 + 2.37 M	.088	.160	14.8	74.2	77	74
l	July 29, 1980	Log API = .38 + 1.90 M	.124	.201	9.47	55.2	73	70

summary of the statistics from cases using the day-night technique. Table 3 gives the statistics from the cases using the afternoon temperature alone technique. As can be seen from a brief study of the R^2 values from the tables, the accuracy of the inference of soil moisture appears to be more case dependent than technique dependent. Moreover, the R^2 of the correlation of M and LOG API appears to be dependent on wind speed and low level humidity, as taken from synoptic data, to some extent.

Figure 53 shows the regression equations obtained from the use of the morning temperature rise technique. Figure 54 represents the combined results of the regression between M and LOG API for both the day-night technique and the afternoon image only technique. In both figures there is considerable variability in the equation found. However, except for case c, where a cold front was present, and case e, where large amounts of rain had recently fallen over the entire area, all of the equations show a similar slope (approximately 2) and intercept within an accuracy of about plus or minus 20% of the total range of M.

At this point the reader should be cautioned that, although there appears to be somewhat of a consistent relationship between M and LOG API and the application of this result is sure to be site specific and dependent on the time of year. In addition, the relationship should only be applied as a gross measurement, since the low R^2 for the cases implies that there many small scale processes taking place that cannot be accounted for in this method of soil moisture assessment.

Five cases using the "day-night" techniques were selected to be presented in a time series comparison of two sub-areas within the main

TABLE 3

Summary of regression statistics for cases using the "Single Afternoon Image" Technique

Case	Date	Regression Equation	Standard Deviation Intercept	Standard Deviation Slope	T-Ratio Slope	R^2%	Number of Points	% of Image Clear
f	June 27, 1980	Log API = 1.23 + 2.03 M	.148	.283	7.15	37.6	84	81
1	July 29, 1980	Log API = .38 + 1.90 M	.124	.201	9.47	55.2	73	70

TABLE 4

Listing of cases, technique used and satellite overpass times

Case	Date	Time(s) of Satellite Overpass Central Standard (Local Time)	Technique Used to Evaluate Moisture Availability	Remarks
a	July 15, 1978	0800 1300	"Morning temperature rise"	Light winds, some clouds, moderate low-level humidity
b	July 27, 1978	0830 1400	"Morning temperature rise"	Light winds, high thin cirrus, high humidity
c	July 1, 1980	0830 1400	"Morning temperature rise"	Cold front over area
d	July 14, 1980	0800 1400	"Morning temperature rise"	Strong winds, low humidity
e	Aug 23, 1980	0800 1400	"Morning temperature rise"	Moderate winds, high humidity
f	June 27, 1980	1300	"Single afternoon image"	Morning clouds, strong winds, low humidity
g	June 30, 1980	1300 0000	"Day-Night"	Strong winds, high humidity
h	July 6, 1980	1330 0000	"Day-Night"	Moderate winds moderate humidity
i	July 13, 1980	1400 0000	"Day-Night"	Strong winds, low humidity
j	July 22, 1980	1400 0000	"Day-Night"	Light winds, low humidity
k	July 28, 1980	1400 0000	"Day-Night"	Light winds, moderate humidity
l	July 29, 1980	1400	"Single afternoon image"	Morning clouds moderate winds, low humidity

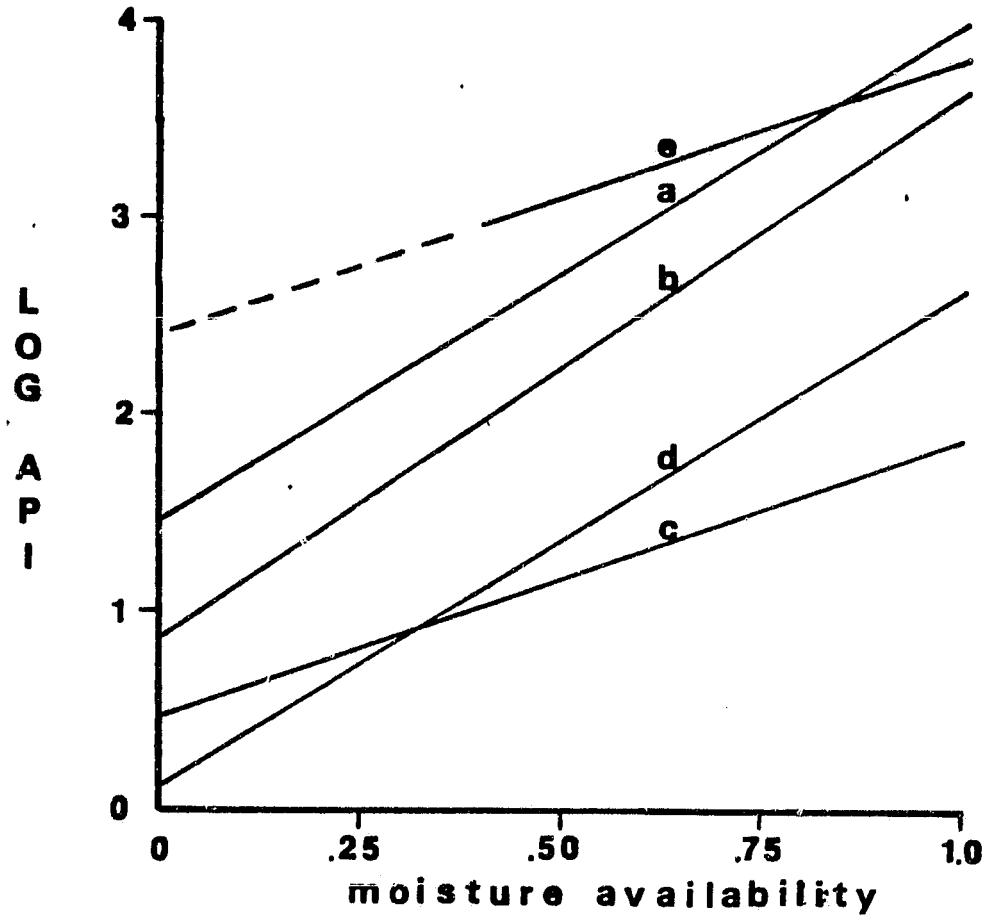

Figure 53. Results from correlation of satellite derived moisture availability and Log Api calculated from rainfall data for cases using the morning temperature rise technique.

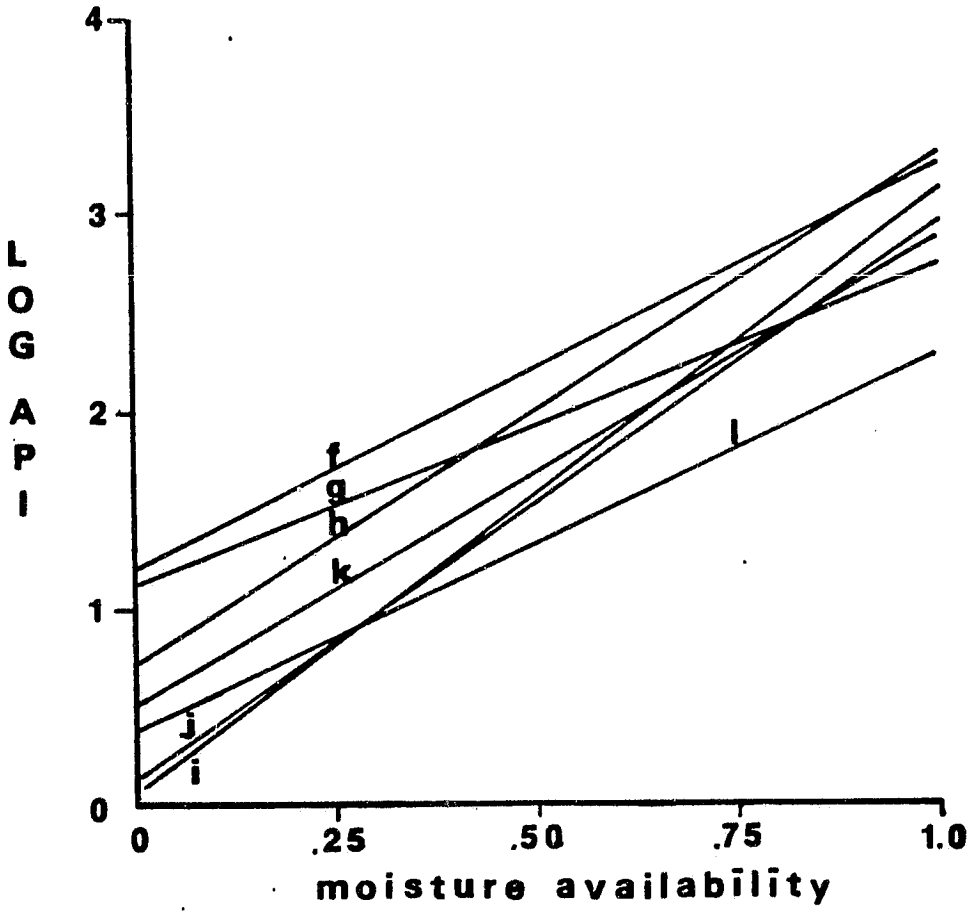

Figure 54. Results from correlation of satellite derived moisture availability and Log API calculated from rainfall data for cases using either the "Day-Night" Technique of the single afternoon image technique.

study area. The sub-areas were, for the most part, on opposite sides of the rainfall gradient present across Kansas. The location of the "wet" and "dry" sub-areas are shown in Fig. 55.

The time series in Figure 56 gives the range of API and satellite derived M values within the two sub-areas for the five cases. A range of API values are taken because of uncertainty due to the widely spaced network of rainfall stations and the smoothing necessary to obtain analyses of API from them. M values are also given in the form of a range because of the noise present in their analyses.

4.6 Sources of Error

In all of the techniques used to infer soil moisture, an accurate measure of surface temperature is essential. However, a satellite's indirect measure of temperature is subject to error from several sources.

Clouds are the greatest obstacle in determining surface temperature from longwave IR satellite data. In fact, the main use of the GOES IR band is for observing the extent of cloud coverage and in determining cloud heights. The presence of clouds can be obvious as in the case of a large cumulioform clouds whose radiating temperature is much lower that of surrounding pixels. However, the effects of small fair weather cumulus and thin layers of cirrus are difficult, if not impossible, to isolate. These clouds blend in with surface emissions causing a lower temperature to be recorded for any pixel containing these clouds.

Water vapor in the lower atmosphere is another source of error in assessment of surface temperature. To some extent a water vapor

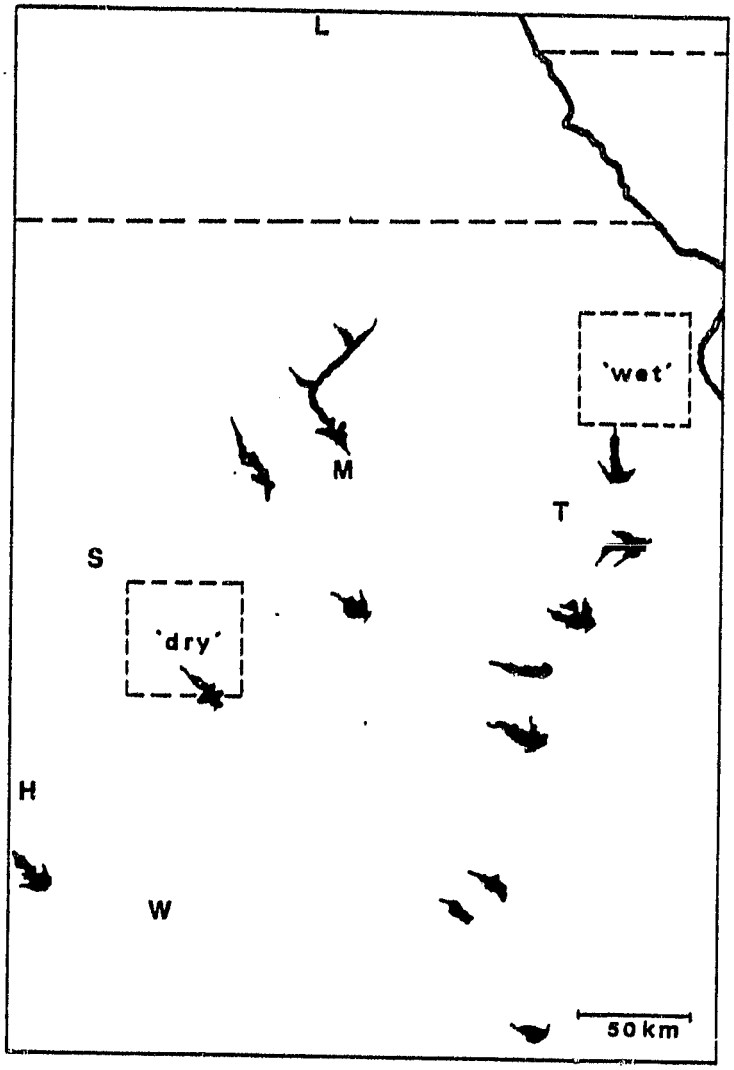

Figure 55. Location of "wet" and "dry" sub-areas.

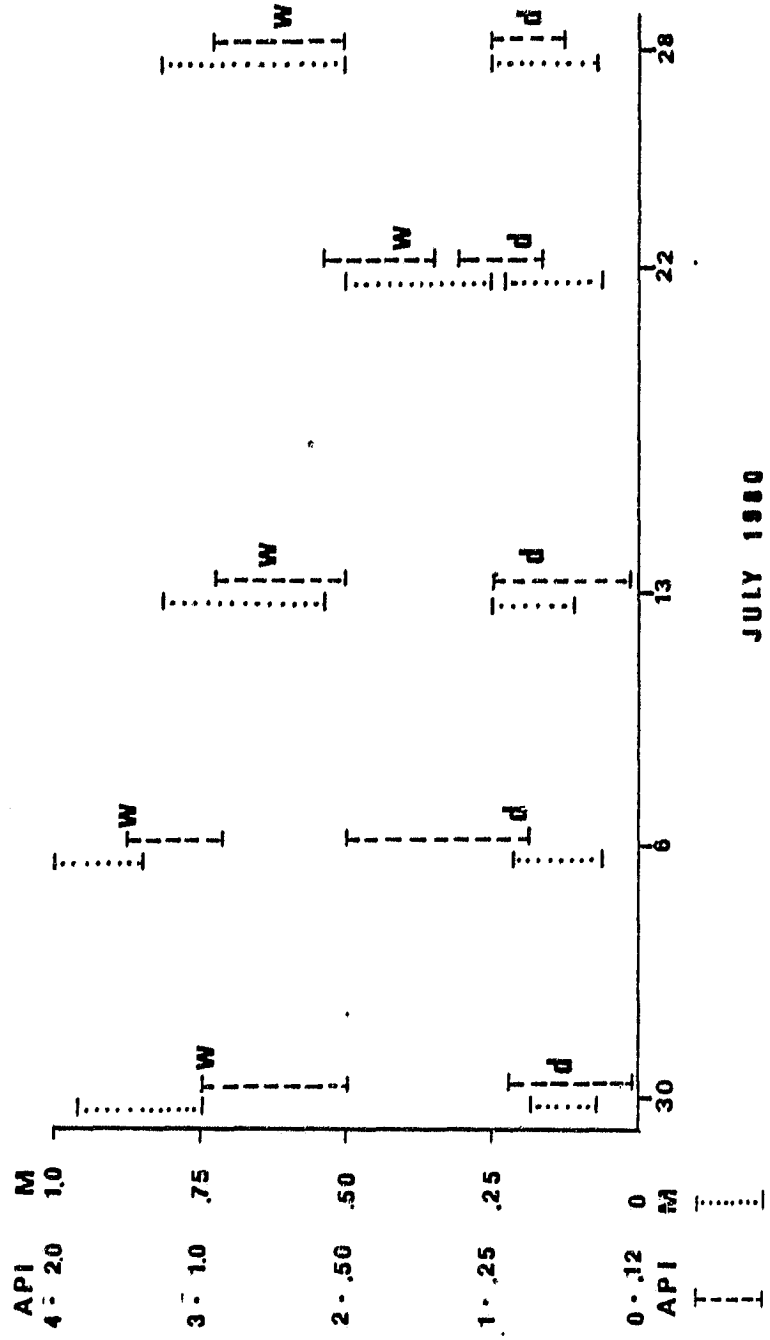

Figure 56. Temporal variations in moisture availability (M-dotted lines) and Log API (dashed lines) for the two "wet" (w) "dry" (d) sub-areas shown in Fig. 55.

correction can be applied to account for this error. This is, in fact, done by the use of a radiative transfer routine developed by Price (Private communication). This routine takes a temperature humildity sounding and provides a linear correction that can be applied to the raw temperature data.

The use of a single correction is only valid for small areas where homogeneity of an air mass exists. For the high summertime temperatures found in this case study, substantial amounts of low level water vapor necessitated the use of a large correction, since the presence of water vapor interfered with transmittance of IR radiation. The correction was found to be in excess of 10 C in some high humidity situations. Also of some concern was the temporal variability in sounding tmeperatures, from which the correction was derived, over a 12 hr period. This variability, represented by the change in the slope of the linear correction equation, was between 5% and 20% for the soundings used.

The surface temperature which is the solution to the one-dimensional PBL model is incapable of describing the horizontal variations in variables such as surface roughness, small-scale wind fluctuations, and vegetation. Spatial temperature variations due to these factors appear in the satellite measurement of surface temperature and are certainly a cause of error in the inference of moisture availability.

Terrain variability can cause spatial variations in temperature for a number of reasons. Slope differences cause the incident angle of solar radiation to depart from that for a flat surface. Elevation can

cause differences in temperature and humidity within the surface layer resulting in heat flux and surface temperature variations.

Over a large region, such as the one studied here, wind speed is certainly not constant. Small-scale differences in wind speed due to inhomogeneous roughness, heat island effects and large time period turbulence (thermal eddies) produce variations in surface heat flux that affect the local surface temperature.

The role of vegetation appears as a paradox in the inference of soil moisture availability (M). No vegetative canopy was included in the model physics, Although actual evaporation is highly dependent on the type and condition of local vegetation. A situation may occur where the top few centimeters of a soil would completely dry out but the vegetation present would extract moisture from deeper layers of the soil resulting in evaporation taking place near the potential rate (an M near 1). For this reason the quantity M does not always imply a measure of soil moisture for a fixed soil depth.

5. CONCLUSIONS AND SUGGESTIONS FOR FUTURE RESEARCH

A method to infer measurements of moisture availability and other surface parameters such as thermal inertia, total evaporation and sensible heat flux from longwave IR temperature data has been developed. This thesis has tried to ascertain the method's value in inferring moisture availability by establishing a correlation between M and the antecedent precipitation, as represented by API. Although API, computed from rainfall data, is not itself a direct measure of surface moisture availability it is expected that a strong relationship must exist between the two. An analysis of twelve cases from 1978 and 1980 over Kansas suggests that over prairie, at least, that there is approximately a linear relationship between the log of the API and moisture availability, which is significant only when averaged over a relatively large area and where there are also large gradients in precipitation.

The method of inferring moisture availability has been shown to be subject to error from various sources, but in spite of these difficulties the tenuous relationship suggests that the satellite possesses some capability for regional-scale soil moisture measurement. The remote determination of moisture availability appears most appropriate with GOES over regional-scale areas of (10^5 to 10^6) sq km, but the derived values of soil moisture are probably significant to within plus or minus one category of four or five relative categories and may not represent absolute values of soil moisture.

In the future, a boundary layer experiment to be conducted in France by the CNET during 1984 may provide ground truth measurements of soil moisture and heat flux which can be compared to satellite derived quantities, thereby providing a greater means for assessing and improving the infrared method.

APPENDIX 1: MODEL IMPROVEMENTS

In the past two years, some improvements have been made to the Carlson et al. (1981) model. The model originally ran on the PSU IBM 370 computer. Since then the model and all of the associated software needed for image processing has been modified and transfered for interactive use on the meteorology department PDP 11/34 minicomptuer (Polansky, 1982). A manual exists documenting the software of this system for any interested persons requiring detailed information on its operation. This appendix will serve as a brief statement describing model improvements made since Carlson et al. (1981).

1) Soil Heat Transfer Computation

Computation of soil heat transfer requires use of second order differencing within the model (see Equation 14). The thickness between soil layers is made to increase exponentially with depth since the temperature gradient within the soil generally is greatest near the surface. In the top layer, between the surface and first soil layer, the small thickness is needed to parameterize soil heat flow accurately. At greater depths small gradients are found requiring less resolution.

The smaller the thickness the greater the chance that the criteria for computational stability will not be satisfied. This criteria is:

$$\frac{\kappa \Delta T}{(\Delta z)^2} < \frac{1}{4} \qquad (23)$$

The time step is set at 240 sec for soil heat transport calculations. The thermal diffusivity (kappa) of the soil was made to vary as a function of the chosen thermal inertia value, accordingly the thickness of the first soil level was made variable satisfying the computational stability criteria. In fixing the depth of the first layer the depth of the bottom layer is also set. The bottom soil layer remains at a constant temperature. Thus, the depth at which the amplitude of a diurnal temperature wave goes to zero becomes a function of the thermal diffusivity. This coresponds to what one finds in nature. A soil with a large thermal diffusivity will have the amplitude of its diurnal wave vanish at a greater depth than that of a soil with a smaller value of kappa (Deardorff, 1978).

2) First Soil Layer Correction

Since the model solves soil heat flux by approximating derivatives by discrete methods, the soil heat flux is underestimated due to the underestimate of the temperature gradient within the first soil layer. To improve upon this we assume that the amplitude of the temperature wave under ideal conditions is a function of depth (Z), diurnal period (w) and thermal diffusivity (k) (Sellers, 1965).

$$T(z) = T_o \, \mathrm{Exp}\left[-z \left(\frac{\omega}{2\kappa}\right)^{1/2}\right] \qquad (24)$$

With this assumption the discrete temperature gradient $(\frac{\Delta T}{\Delta z})$ is multiplied by a correction factor that normally adds about 10% to the discrete derivative to approximate the continuous derivative at the surface.

$$G_o = \frac{2}{1 + \mathrm{Exp}[-\Delta z\ (\frac{\omega}{2\kappa})^{1/2}]} \cdot \lambda \frac{\Delta T}{\Delta z} \approx \lambda \frac{\partial T}{\partial z} \qquad (25)$$

3) Daytime Wind Calculation

In the original model, the daytime wind speed at the top of the surface layer was held constant. To more accurately describe the morning temperature rise a method was developed to allow for a changing daytime wind speed. The inclusion of an observed initial wind profile is introduced. The wind sounding from a rawinsonde station is fitted to the levels of model calculation by means of a cubic spline. Momentum equations are solved to find accelerations resulting from geostrophic adjustments, surface friction and the mixing of momentum from upper level winds. Thus,

$$\frac{\Delta u_i}{\Delta t} = f(v_i - v_{gi}) + \frac{K_{mi+1}(u_{i+1} - u_i)}{\Delta z^2} - \frac{K_{mi}(u_i - u_{i-1})}{\Delta z^2} \qquad (26)$$

$$\frac{\Delta v_i}{\Delta t} = f(u_i - u_{gi}) + \frac{K_{mi+1}(V_{i+1} - V_i)}{\Delta z^2} - \frac{K_{mi}(V_i - V_{i-1})}{\Delta z^2} \qquad (27)$$

These equations are solved at ten levels separated by a spacing of 250 m. The lowest level is handled differently by replacing the last terms of the equations to include effects of surface friction.

$$-\frac{u_*^2 u_1}{w_A \Delta z} - \frac{u_* V_1}{W_a \Delta z} \qquad w_A = U_1^2 + V_1^2 \qquad (28)$$

The mixing coefficients (K_m) are calculated from a method described by O'Brien (1970). These coefficients are determined from values of u* and the Monin-Obukhov length in the surface layer and the height of the mixed layer. These Km values are computed at the 250 m grid levels and also between the grid levels at a spacing of 125 m. From these computed Km values three values are averaged to give a representative Km value for the entire layer between grid levels. In this way the mixing of momentum between grid levels is more accurately represented. The momentum equations are integrated with a time step of 120 sec, twice as often as the basic model step, to insure computational stability during periods when Km values are large.

As a result or the equations, wind speed, which is initially small in the early morning, increases during the morning because of the mixing of momentum from higher level winds which are normally stronger. By afternoon, low level winds reach a quasi-equilibrium between the effects of geostrophic forcing, momentum mixing and surface friction. Therefore, the surface wind speed remains nearly constant approximating its geostrophic value. When the model switches into the nighttime mode the winds from the bottom two daytime layers at a 250 m spacing are interpolated to 10 layers with a 50 m separation for the nighttime wind calculations.

REFERENCES

Balick, L.K., L.E. Link, R.K. Scoggins, Thermal Modeling of Terrain Surface Elements, Technical Report E1-81-2, Environmental Laboratory, U.S. Army Engineering Waterways Experiment Station, Vicksburg, Miss.

Benjamin, S.G., 1983, Some Effects of Surface Heating and Topography on the Regional Severe Storm Environment. Ph.D. Dissertation, Department of Meteorology, The Pennsylvania tate University, State College, PA.

Carlson, T.N. and F.E. Boland, 1978, Analysis of urban-rural canopy using a surface heat flux/temperature model. Journal Applied Meteorology, 17: 998-1013.

Carlson, T.N., J.K. Dodd, S.G. Benjamiln and J.N. Cooper, 1981, Satellite estimation of surface energy balance, moisture availability, and thermal inertia. Journal Applied Meteorology, 20: 67-87.

Deardorf, J.W., A parameterization of ground-surface moisture content for use in atmospheric prediction models. Journal of Applied Meteorology, 16: 1182-1185.

Degloire, J. and Megier, J., 1979: Mapping thermal inertia, soil moisture and evaporation from aircraft day and night thermal data. Proc. of the 13th International Symposium on Remote Sensing of the Environment. Environmental Research Institute of Michcigan, Ann Arbor, pp. 1015-1027.

Dodd, J.K., Determination of surface characteristics and energy budget over an urban-rural area using satellite data and a boundary layer model. M.S. Thesis, Department of Meteorology, The Pennsylvania State University, 1979.

Eagleman, J.R. and W.C. Lin, "Detection of soil moisture by a 21 cm passive radiometer," Journal of Geophysical Research, 81, 3660-3666, 1976.

Heilman, J.L., V.I. Myers, D.G. Moore, T.J. Schmugge and D.B. Friedman, Soil Moisture Workshop, NASA Conference Publication 2073, January 17-19, 1978.

Idso, S.B., R.D. Jacakson and R.J. Reginaton, Compensation for environmental variability in the thermal inertia approach to remote sensing of soil moisture, Journal of Applied Meteorology, 15: 811-817.

REFERENCES (Continued)

Kocin, P.J., 1979, Remote Estimation of Surface Moisture Over a Watershed, M.S. Thesis, Department of Meteorology, The Pennsylvania State University.

Miller, I., J.E. Freund, 1977, Probability and Statistics for Engineers, 2nd edition, Prentice-Hall, Inc., Englewood Cliffs, NJ.

Oke, T.R., 1978, Boundary Layer Climates, Methven and Co. Ltd., Halsted Press Book, John Wiley and Sons, New York.

Polansky, A.C., 1982, A Method for Diagnosing Surface Parameters Using Geostationary Satellite Imagery and a Boundary-Layer Model, M.S. Thesis, Department of Meteorology, The Pennsylvania State University.

Price, J.C., Thermal inertia mapping: A new view of the earth. J. Geophysical Res., 82: 2582-2590 (1977).

Price, J.C., The potential of remotely sensed thermal infrared data to infer surfer surface soil moisture and evaporation,. Water Resources Research. 16: 787-795, 1980.

Rosema, A. and J.H. Bijeveld, P. Reininger and G. Tassone, K. Blyth and R.J. Gurney, 1978, "Tell-Us" a combined surface tempeature, soil moisture, and evaporation mapping approach. Proc. of the 12th Int. Symp. on Remote Sensing of the Environment. Environmental Research Institute of Michigan, Ann Arbor.

Ryan, T.A., Jr., B.L. Joiner, and B.F. Ryan, 1976, MINITAB Student Handbook. Duxbury Press, North Scituate, MA, 341 pp.

Saxton, K.E. and A.T. Lenz, Antecedent Retention Indexes Predict Soil Moisture. Journal of the Hydraulics Division, Proceedings of the Civil Engineers, July 1967.

Sellers, W.D., Physical climatology. Univ. of Chicago Press, Chicago, 1965.

Soer, G.J.R., 1980, Estimation of regional evapotranspiration and soil moisture conditions using remotely sensed surface temperatures. Remote Sensing of the Environment. 9: 27-45.

Wetzel, P.J. and Atlas, D., 1981, Inference of precipitation through thermal infrared measurements of soil moisture. Precipitation Measurements from Space Workshop Report, 1981. Atlas, D. and Thiele, O.W., Ed., Goddard Laboratory for Atmospheric Sci., Goddard Space Flight Center, Greenbelt, MD, pp. D-170 to D-172.

REFERENCES (Continued)

Wetzel, P.J. and D. Atlas, 1983, Inference of Soil Moisture from Geosynchronous Satellite Infrared Observations to be published. Goddard Laboratory for Atmospheric Sci. NASA /Goddard Space Flight Center, Greenbelt, MD.